energies

MDPI

Article

Advanced Energy Management in a Sustainable Integrated Hybrid Power Network Using a Computational Intelligence Control Strategy

Muhammad Usman Riaz [1,*], Suheel Abdullah Malik [1], Amil Daraz [2,3], Hasan Alrajhi [4], Ahmed N. M. Alahmadi [4] and Abdul Rahman Afzal [5,*]

[1] Department of Electrical and Computer Engineering, International Islamic University Islamabad, Islamabad 44000, Pakistan; suheel.abdullah@iiu.edu.pk
[2] College of Information Science and Electronic Engineering, Zhejiang University, Hangzhou 310027, China; amil.daraz@zju.edu.cn
[3] MEU Research Unit, Middle East University, Amman 11831, Jordan
[4] Department of Electrical Engineering, Umm Al-Qura University, Makkah 21955, Saudi Arabia; hkrajhi@uqu.edu.sa (H.A.); anmahmadi@uqu.edu.sa (A.N.M.A.)
[5] Department of Industrial Engineering, University of Business and Technology (UBT), Jeddah 23847, Saudi Arabia
* Correspondence: muhammad.phdee34@iiu.edu.pk or engineerusmanriaz@outlook.com (M.U.R.); a.afzal@ubt.edu.sa (A.R.A.)

Abstract: The primary goal of a power distribution system is to provide nominal voltages and power with minimal losses to meet consumer demands under various load conditions. In the distribution system, power loss and voltage uncertainty are the common challenges. However, these issues can be resolved by integrating distributed generation (DG) units into the distribution network, which improves the overall power quality of the network. If a DG unit with an appropriate size is not inserted at the appropriate location, it might have an adverse impact on the power system's operation. Due to the arbitrary incorporation of DG units, some issues occur such as more fluctuations in voltage, power losses, and instability, which have been observed in power distribution networks (DNs). To address these problems, it is essential to optimize the placement and sizing of DG units to balance voltage variations, reduce power losses, and improve stability. An efficient and reliable strategy is always required for this purpose. Ensuring more stable, safer, and dependable power system operation requires careful examination of the optimal size and location of DG units when integrated into the network. As a result, DG should be integrated with power networks in the most efficient way possible to enhance power dependability, quality, and performance by reducing power losses and improving the voltage profile. In order to improve the performance of the distribution system by using optimal DG integration, there are several optimization techniques to take into consideration. Computational-intelligence-based optimization is one of the best options for finding the optimal solution. In this research work, a computational intelligence approach is proposed to find the appropriate sizes and optimal placements of newly introduced different types of DGs into a network with an optimized multi-objective framework. This framework prioritizes stability, minimizes power losses, and improves voltage profiles. This proposed method is simple, robust, and efficient, and converges faster than conventional techniques, making it a powerful tool of inspiration for efficient optimization. In order to check the validity of the proposed technique standard IEEE 14-bus and 30-bus benchmark test systems are considered, and the performance and feasibility of the proposed framework are analyzed and tested on them. Detailed simulations have been performed in "MATLAB", and the results show that the proposed method enhances the performance of the power system more efficiently as compared to conventional methods.

Keywords: distributed generation (DG); optimal DG location; optimal sizing; Fitness-Dependent Optimizer (FDO); distributed network (DN); renewable energy sources; distribution system (DS); optimization; control; evolutionary computation

Citation: Riaz, M.U.; Malik, S.A.; Daraz, A.; Alrajhi, H.; Alahmadi, A.N.M.; Afzal, A.R. Advanced Energy Management in a Sustainable Integrated Hybrid Power Network Using a Computational Intelligence Control Strategy. *Energies* **2024**, *17*, 5040. https://doi.org/10.3390/en17205040

Academic Editors: Wencong Su and Guilherme Vieira Hollweg

Received: 3 September 2024
Revised: 3 October 2024
Accepted: 4 October 2024
Published: 10 October 2024

1. Introduction

With the increasing electricity demand, the energy crisis has become one of the most important challenges/issues faced today around the world. Dispersed generation, which is also known as distributed generation (DG), has become a major economical and common source of energy for electricity generation because it helps to overcome the increasing load demand. DG represents a modern approach in power distribution systems to handle the increasing demand for electric energy. It refers to small-scale power generation units located near the load, such as photovoltaics (PVs), solar panels, wind turbines, synchronous and induction generators, micro-turbines, and fuel cells [1,2]. Smart grids are also natural expansions of decentralized generation. DG is an essential component of smart grids, enables them to generate decentralized power on-site or near the load, helps to reduce peak loads, and improves the management systems of central power grids [3].

Distributed generation is becoming more popular in power systems due to its numerous benefits, including improvements in voltage profiles and reductions in power losses. It also improves the power quality of the network. Similarly, when DG is integrated, there is no need to upgrade the transmission lines of the power network. This eliminates the need to expand transmission and distribution network capacity, thereby saving on infrastructure costs while reducing transmission and distribution losses typically associated with centralized power generation. As a result, reliance on central generation (CG) is minimized. The impacts of DG integration are generally on power losses, voltage profiles, load demands, and the reliability and stability of the power systems, which are significantly considered important for power systems development and planning. Efforts for effectively utilizing renewable energy sources based on DG, like wind power and PV–solar power, have increased as awareness of energy issues, including environmental pollution and global warming, has grown. In addition, DG also facilitates the integration of modern renewable energy sources into power distribution systems, helping to reduce greenhouse gas emissions and promote the use of sustainable energy in practice for an effective electricity supply. Modern DG-based renewable energy sources produce high-quality, environmentally friendly, cost-effective, and reliable power compared to conventional energy sources. These sources help address energy problems related to pollution and climate change [4]. The optimal placement of DG plays a crucial role in increasing its penetration within distribution networks. Achieving the greatest benefits from DG integration requires selecting both the optimal location and size of DG units, which can significantly reduce power losses and improve voltage profiles [5].

Furthermore, studies have shown that using multiple DG units instead of a single unit can reduce power losses to a greater extent and enhance voltage profiles. Multiple DG units also reduce the burden on individual branches, minimizing branch power losses. Therefore, integrating multiple DG units results in greater reductions in losses and more substantial improvements in voltage profiles compared to using a single DG unit. To balance voltage variations, reduce power losses, and overcome stability issues, the strategic placement and sizing of multiple DG units offer a credible solution [6].

The impact of DG integration is generally on power losses, voltage profiles, load demand, and the reliability and stability of power systems, which are significantly considered important for power systems development and planning. DG insertion into the power systems has several kinds of impacts on the electrical power systems, but because of its plug-and-play capabilities, operational flexibility, and other advantages, it is an attractive option for future power systems. The primary benefit of connecting the DG is to increase the overall efficiency of the electrical power systems without requiring major alterations to the existing infrastructure. Transmission losses, which occur when electricity is transmitted over long distances, typically range from 5% to 10% of the transmitted power. These losses arise from various factors like the reactive nature of certain components, bulk resistance, connection losses, etc. Similarly, utility companies charge a bill to consumers for the elec-

tricity cost lost due to how far the transmission lines network is from generating units, which may cause an increase in the electricity generation cost. However, these expenses can be minimized by the integration of DG with an appropriate size at the appropriate placements, which is installed near the load site. Additionally, integrating DG units into power systems can facilitate peak load shaving, improve power quality, and enhance overall stability [7]. DG integration can reduce power losses and improve voltage profile areas where service providers have issues with voltage dips and blackouts. In such areas, where service providers are concerned about voltage dips and blackouts, the injection of DG may reduce the power losses and compensate for the voltage drop. Incorporating DG into a power system can improve the voltage profile and minimize power losses, but where they will be installed in the network depends on the size, type, and ideal placement of DG units. The optimal integration of modern renewable energy sources (MRES) based on DG can help enhance the reliability, efficiency, and sustainability of the power system. These MRES-based DG units, i.e., solar, and wind power, etc., can also help reduce the effects of greenhouse gas emissions and mitigate climate change, leading to improved energy efficiency and lower operating costs. Additionally, DG can provide energy independence to communities or facilities located in remote or off-grid areas, decreasing reliance on fossil fuels while promoting the use of renewable energy sources. However, if a DG unit of the appropriate size is not inserted in the proper location, it might have an adverse impact on the voltage profile, increase power losses, and compromise the reliability and operation of the power system [8].

However, the improper integration of DG into power networks is found to cause an increase in voltage fluctuations, power losses, system instability, and deterioration in power quality. Therefore, the appropriate allocation of DG is essential for improving the performance of the distribution networks (DN). Optimal integration of DG into existing power systems helps improve voltage profile and reduce power losses, ultimately improving the overall quality, stability, and efficiency of the power system for both non-uniform and non-unity power factor distributed loads [9]. Integration of DG into existing power system infrastructure can cause challenging issues due to the intermittency and variability of modern renewable energy sources. Consequently, advanced power system management and control strategies are essential to ensuring the reliability and stability of the power system. Additionally, issues related to weak voltage profiles and power losses in distribution networks are significant factors that motivate researchers to explore further optimal solutions [10].

This research aims to propose an effective strategy for optimal DG integration into a power distribution network. This goal is to determine the optimal placement and sizing of DG units to improve voltage profiles, reduce power losses, and enhance the stability of the distribution network. Hence, it is extremely important to study the appropriate sizing and location of DG units within the network to ensure more stable, safer, and reliable power system operations. Voltage profiles and power losses, which are based on the sizes and placements of DG units, play a key role in achieving overall optimization. The optimal placement and sizing of DG can be determined using various optimization techniques. The optimization problem is formulated based on load flow equations, subject to constraints, and objective functions, and is then solved using optimization methods. In order to optimize the DG-integrated hybrid power grid network, there are several optimization techniques taken into consideration, but computational-intelligence-based optimization is one of the most effective approaches for identifying the optimal solution [11,12].

In the literature discussed in the past, several techniques have been proposed and developed for solving DG placement problems, and a few of the studies have been discussed and illustrated as follows. In reference [13], the author proposed the use of the "Genetic Algorithm" (GA) for the DG placement problems. This method is tested on the semi-urban 37-bus distribution network (DN), and its results demonstrate its validity. However, there are a lot of complications when this approach is utilized for larger distribution networks. In [14], the author proposed a Multi-Objective Index (MOI) technique for DG allocation,

which accommodates various load models. This technique is applied to the standard IEEE 37-bus systems. In [15], the authors presented another technique for optimal DG placement and sizing, utilizing the Shuffled Frog Leap Algorithm (SFLA). The validity of this method is verified on the IEEE 33-bus and IEEE 15-bus systems. In [16], the author presented the Fuzzy Adaptation Technique (FAT) based on Evolutionary Programming to determine the optimal capacity and allocation of DG units. In [17], the author used the "Artificial Bee Colony" (ABC) algorithm, which is based on a "meta-heuristic" approach, to identify the best locations and sizes of distributed energy sources. In [18], the Global Search Algorithm (GSA) is used for the optimal allocation and capacity of determination of Distributed Energy Resources. This approach is tested on the standard IEEE 33-bus and 69-bus systems. In [19], a Shuffled Frog Leap Algorithm (SFLA), which incorporates a cooperative fuzzy sustaining method, is employed to solve optimization problems, with the IEEE 69-bus system used for the evaluation of the suggested system. In [20], the paper proposed a hybrid technique that combines the "SFLA" and "BAT" algorithms. In [21], the authors introduced a unique and efficient optimization method for DG placement and sizing, known as the Shuffled ABC Algorithm (SHABC). This method combines the strengths of both the SFLA and ABC algorithms to enhance overall search efficiency through a hybrid approach. In [22], the author proposed a modern, higher-level, nature-inspired algorithm, Simulated Annealing (SA), for DG integration into distribution networks. This approach considers economic, technological, and environmental factors, as well as uncertainty. In [23], the author addressed the issues presented in [22] by proposing a nonlinear programming technique for determining the optimal location and sizing of DG units. A numerical problem based on differential evolution was utilized to resolve these issues. However, this approach also faces significant complications when applied to large distribution networks. In [24], an analysis was performed on the presence of DG and its impact on power system performance using nature-inspired techniques such as the "Artificial Bee Colony" (ABC) and "Cuckoo Search Algorithm" (CSA). These techniques were employed to determine the optimal placement and sizing of DG units and to improve the efficiency of radial distribution networks. The Firefly Algorithm (FA) demonstrated exceptional optimization capabilities by solving non-linear dispatch problems and providing optimal solutions for systems with multiple generations [25–27]. The Hybrid Firefly–JAYA Algorithm is used to optimize power flow while considering wind and solar power generation [28]. The Teaching–Learning-Based Optimization Algorithm (TLBOA) with Optimal Power Flow (OPF) successfully minimized dual objective functions, outperforming traditional numerical methods in solving complex optimization problems [29,30]. In [31,32], the author presented the "Genetic Algorithm" (GA) and a hybrid GA [33]. In [34–36], the author presented the "Particle Swarm Optimization" (PSO) technique for optimal DG placement and sizing followed by an improved-PSO [37,38]. A hybrid analytical PSO approach was used in [39], while a hybrid DA-PSO was used in [40]. In [41–43], a hybrid algorithm combining Genetic Algorithm (GA) and Particle Swarm Optimization (PSO), known as GA-PSO, is presented. Various research studies have employed hybrid techniques that combine multiple methods, such as PSO with a Fuzzy Approach in [44], discrete PSO–Optimal Power Flow (PSO-OPF) in [45], hybrid PSO–Gradient Search Strategy (PSO-GSS) in [46], and hybrid Gravitational Search Algorithm–Improved PSO (GSA-IPSO) in [47], all aimed at determining the optimal DG placement and sizing. In [48,49], the system performance with multiple integrated DG units was analyzed using standard IEEE bus test systems, employing nature-inspired computational approaches to enhance voltage profiles and minimize power losses. Optimal DG allocation in a distribution network (DN) is a challenging optimization problem, requiring the identification of the best DG location and size to reduce power system losses and improve voltage stability [50]. Recently, several studies have proposed various algorithms and optimization techniques to identify optimal solutions for DG-integrated power systems. After comprehensive literature studies, it is evident that researchers continued to focus on the optimization problems for DG-interconnected systems, such as allocation and sizing, since they offer numerous advantages from an economical point

of view. Conventional methods are almost completely obsolete, and the new modern approaches are used with many variants of intelligence-based techniques due to their simplicity, robustness, high search efficiency, and taking less computational time and effort.

Therefore, in this research, a new computational intelligence (CI) optimization approach, called the hybrid Modified Fitness-Dependent Optimizer (MFDO), is proposed to optimize DG integration in the hybrid power network. The MFDO is employed for solving the DG "placement" and "sizing" optimization problems to minimize power losses, improve the voltage profile, and enhance power reliability and power quality in the distribution network (DN) [51]. The robustness of the MFDO technique in efficiently optimizing DN is a key factor in its selection. This technique has very satisfactory performance and takes minimum time to achieve the optimum solutions. Additionally, it is capable of solving complex optimization problems with low computational time, even for large power systems, and does so with a reduced number of iterations [52–57]. The MFDO has more competitive results as compared to other metaheuristic algorithms, making it applicable for solving a wide range of real-world engineering problems [58–60]. However, while the original FDO swarm intelligence technique is useful for optimization, it has certain limitations. Both FDO and IFDO demonstrate competitive performance, but they suffer from several key issues, including premature convergence, poor exploitation, an imbalance of exploitation and exploration, a slow convergence rate, and insufficient memory allocation. Consequently, modifications to the FDO are introduced to resolve the FDO and IFDO issues such as premature convergence, the slow convergence rate, poor exploitability, insufficient memory allocation, prediction accuracy, and refining solutions. The modified FDO (MFDO) optimization technique is more efficient, and robust, which is an enhanced version of original the FDO. It incorporates improvements such as a modified weight factor, pace updating mechanism, fitness weight adjustment, and optimized hive and scout bee position and velocity values to resolve the FDO and IFDO issues, thereby increasing prediction accuracy and solution precision. The MFDO enhances the exploration and exploitation capabilities; it can be readily constrained into local optima, converges more quickly, and performs better than FDO and IFDO algorithms. This makes it well suited for solving complex problems and providing optimal solutions.

In this research work, the power distribution network (DN) is optimized using the proposed control strategy in conjunction with the MFDO technique. This approach effectively minimizes the power losses and improves the system's voltage profile by integrating various types of DG, including type-1, type-2, type-3, and type-4. This is also capable of finding optimal sizes and locations for integrating single or multiple DG units, within non-uniformly and heavily overloaded distribution networks [61–63]. To identify the best positions for DG allocation, several multi-objective functions are considered essential in this work. The proposed method has been successfully implemented under conditions of randomly connected, and heavily varying loads at low power factor (PF) levels, and accommodating both single and multiple DG units. Additionally, the performance of the proposed method is compared with other techniques, to verify its validity and effectiveness. To evaluate its validity and effectiveness, the IEEE 14-bus and 30-bus test systems have been considered as a case study.

The main contribution of this study is as follows:

- A newly developed nature-inspired optimization technique, i.e., Fitness-Dependent Optimizer (FDO), and its modified and enhanced variant, the so-called Modified Fitness-Dependent Optimizer (MFDO), are proposed and implemented for power system optimization problems within a multi-objective framework.
- The improvement proposed in the optimization methodology hybridizes the optimization algorithm with a new fitness-dependent strategy, which includes optimized updating pace, weight factors, and hybrid sine cosine parameters integrated into the MFDO to enhance its performance. This approach indicates that the concept of advanced techniques theory is incorporated into the proposed method to improve the performance of the convergence rate, reduce simulation time, and enhance the

quality of the solution, etc., ultimately facilitating the effective attainment of the optimal solution.

- In this work, a multi-objective weighted sum approach is employed to effectively optimize the multi-objective functions by balancing the various single-objective functions using relative weights.
- The integration of multiple DG into an existing electrical power network is optimized under different operating modes to maximize the technical benefits of DG across a range of load levels. This research proposes a computational intelligence approach characterized by outstanding search capabilities to determine the optimal placement, sizing, type, and number of DG units. Unlike previous studies that focused solely on optimal DG placement and sizing, this study offers a comprehensive solution by providing optimal settings for DG placement, sizing, type, and number.
- The power distribution network (DN) is optimized using the proposed hybrid MFDO technique, which effectively minimizes power losses and improves the voltage profile by integrating different types of DG, including type-1, type-2, type-3, and type-4.
- The MFDO is capable of identifying appropriate sizes and optimal locations for single or multiple DG units to be integrated into non-uniformly and heavily loaded DNs.
- The overall performance of the power distribution network (DN) can be significantly improved when the optimal power factor operating mode for DG is selected. Previous research has often overlooked this aspect, primarily focusing on DG operating under unity power factor conditions. However, advancements in technology now allow DG units equipped with power electronic inverters to operate effectively at desired power factor modes. Our proposed method addresses this issue by successfully managing randomly connected, heavily varying loads under low power factor conditions for both single and multiple DG units. The superiority of the proposed approach over other existing methods was tested and compared. To evaluate the robustness and validity of the MFDO, its results are compared with benchmarked against several algorithms, including FDO, Hybrid GA-IPSO, IPSO, PSO, and GA.
- To check the method's validity and effectiveness, the IEEE 14-bus and 30-bus test systems have been considered as a case study.
- This study can help power generation and distribution companies, such as IPPs, GENCO, and DISCOs, avoid reimbursements, fines, or penalties, thereby increasing their profit margins through accurate power loss analysis. Additionally, it facilitates the incorporation of renewable energy resources into existing systems.

2. Research Methodology

2.1. Background of Electrical Power System under Case Study

The effectiveness and validity of the proposed method implementation are checked and tested on the IEEE 14-bus and 30-bus test systems. These systems consist of loads, transmission lines, and generator sources. The single-line diagram of the 14-IEEE bus system is shown in Figure 1a, while the single-line diagram of the IEEE 30-bus system is shown in Figure 1b, respectively. These test systems are preferred due to their easy data availability and simplicity. They are also easier to handle, making it convenient to compare results across different studies and optimization methods. In contrast, larger IEEE test systems feature more complex distribution network structures. The IEEE 14-bus and 30-bus systems are considered small- to medium-sized test systems, including both transmission and distribution network models. They are manageable when it comes to debugging and analyzing results. Due to their smaller size and lower complexity, these systems exhibit high computational efficiency, generally run faster, and require fewer computational resources and less execution time. Larger test systems, on the other hand, demand more advanced computational tools, resources, and execution time. Simulink software, such as MATLAB, has been used for modeling and analyzing the benchmark test systems, with simulations performed accordingly. The proposed optimization method was

evaluated in the MATLAB 2018 version environment and executed on a personal computer (Intel Core™ Duo 2.66 GHz, 2 GB RAM).

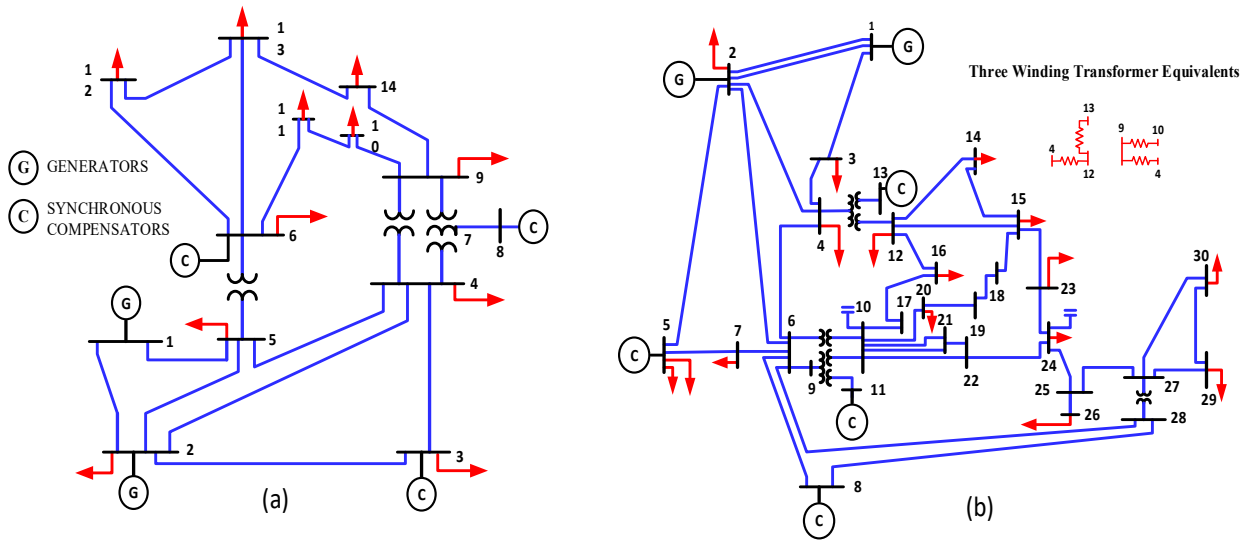

Figure 1. The proposed advanced energy management based on IEEE benchmark tested systems (**a**) IEEE 14-bus network and (**b**) IEEE 30-bus network.

2.2. Methodology for DG Optimal Placement and Sizing

To achieve the optimization of DN, the study proposes a mathematical model, problem formulation, and solution technique to identify suitable possible allocation and sizing of DG units that reduce the power losses and deviation in voltages while ensuring the stability of the network, as shown in Figure 2.

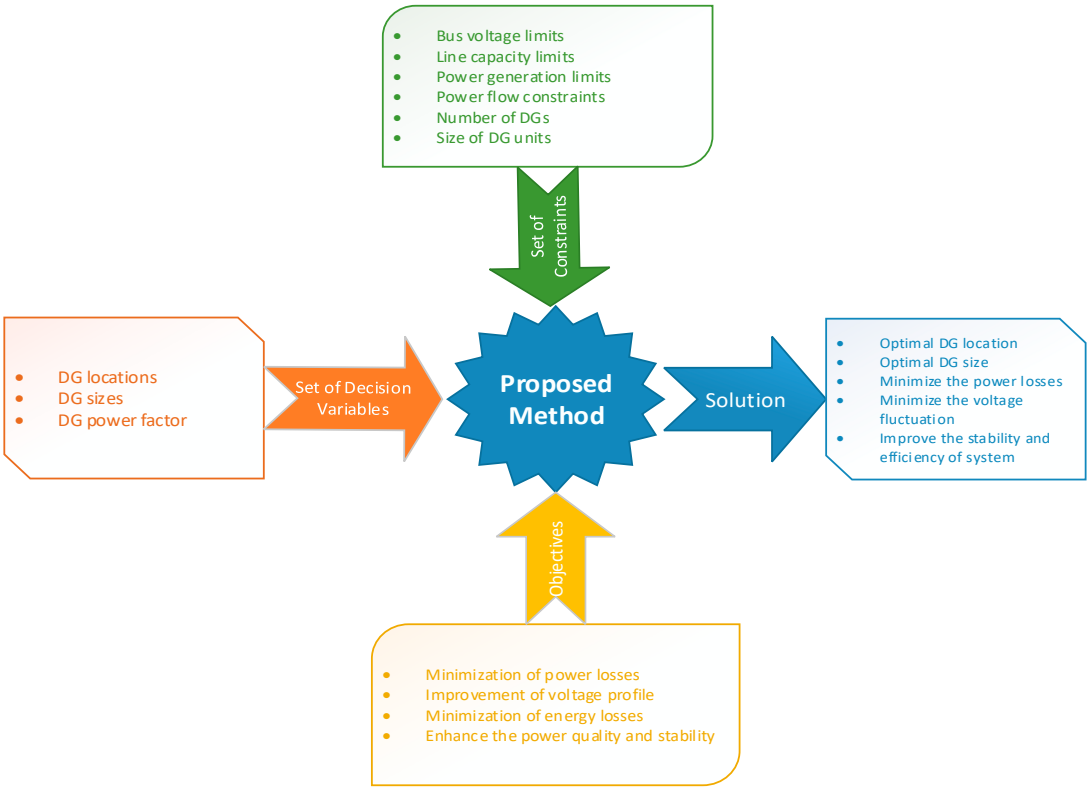

Figure 2. Overview of methodology for DG optimal placement and sizing.

2.3. Mathematical Model and Problem Formulation

Before and after the installation of DG at any arbitrary location in the existing network, the power losses $P_{(Loss)}$ can be calculated by the given equations, respectively. Power loss before DG occurs between the '*i*' and '$i + 1$' buses.

$$P_{i+1} = P_i - P_{Loss,i+1} - (P_{Li+1}) \tag{1}$$

$$P_{Loss(i,i+1)} = \frac{R_i}{V_i^2}.(P_i^2 + Q_i^2) \tag{2}$$

$$P_{i+1} = P_i - \frac{R_i}{V_i^2}.(P_i^2 + Q_i^2) - (P_{Li+1}) \tag{3}$$

Then, the total power loss of the power network such as $P_{T(Loss)}$ can be calculated by summing up as in Equation (4) [47].

$$P_{T,Loss(i,i+1)} = \sum_{i=1}^{n} \left\{ \frac{R_i}{V_i^2} * (P_i^2 + Q_i^2) \right\} \tag{4}$$

After the integration of DG units, the total power loss $P_{T(Loss)}$ may be determined by modified equations as shown below (5), and the model shown in Figure 3.

$$P_{DG,TLoss(i,i+1)} = \frac{R_i}{V_i^2} * (P_i^2 + Q_i^2) + \frac{R_i}{V_i^2} * (\alpha - \beta) \tag{5}$$

where; $\alpha = {P_{DG}}^2 + {Q_{DG}}^2$, $\beta = 2P_i \cdot P_{DG} - 2Q_i \cdot Q_{DG}$.

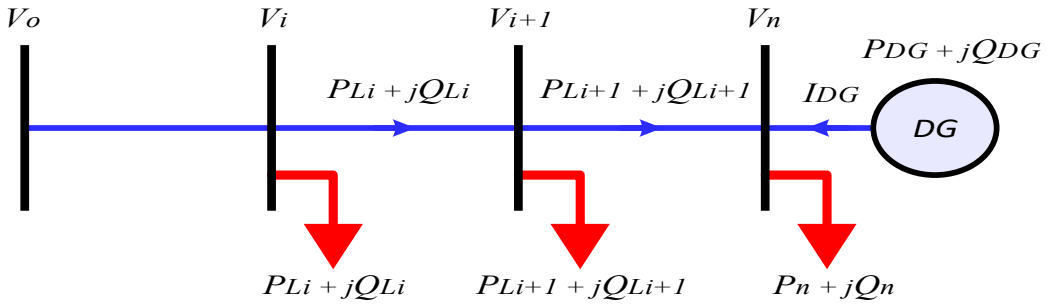

Figure 3. Typical power distribution network with DG.

P_{DG} is donated as the DG real output power for i^{th} DG and defined as $P_{DGi} = [P_{DG1}, P_{DG2}, P_{DG3}, \ldots\ldots\ldots\ldots, P_{DGn}]$ and Q_{DG} is donated as the DG reactive output power for i^{th} DG and defined as $Q_{DGi} = [Q_{DG1}, Q_{DG2}, Q_{DG3}, \ldots\ldots\ldots\ldots, Q_{DGn}]$.

2.4. Modeling of Modern Renewable-Energy-Source-Based Distributed Generation Units

Modern hybrid DG based on Renewable Energy Sources (MRESs) are electric energy resources that can provide energy solutions to clients or end users that are more environmentally friendly, cost-effective, highly reliable, and more efficient than conventional energy sources. The uncertainty of sources such as wind and solar DG is considered in the proposed network. The MRES based on the DG-integrated hybrid power system is shown in Figure 4.

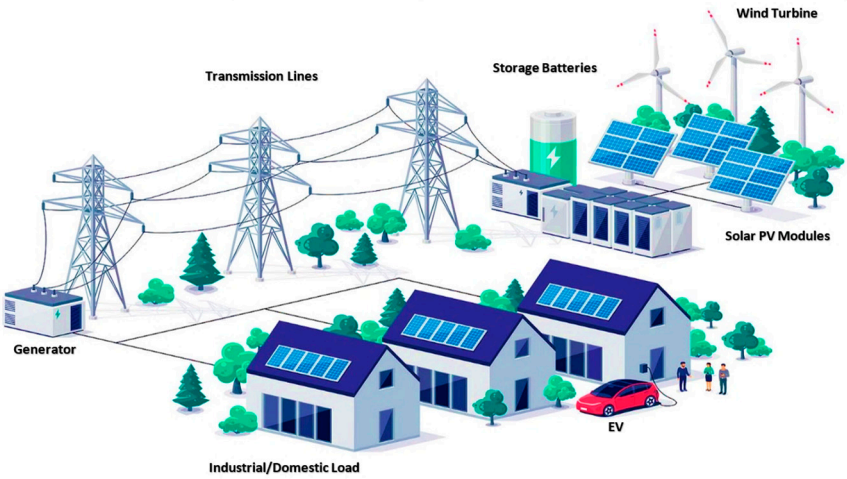

Figure 4. Modern energy sources integrated hybrid power network model.

(i) Wind Turbine DG Model.
The wind turbine DG modeling consists of the following steps:

(a) Wind turbine output power: The output power of a wind-based DG can be represented by a function that relates the speed of wind to the generated power. The output power of a wind turbine is typically modeled using the power coefficient curve or turbine-specific power curve. It relates the wind speed to the generated power and can be represented by an equation as follows:

$$P_{wind} = f(v) = 0.5 \times \rho \times A \times C_p \times V^3 \quad (6)$$

where A, Cp, ρ, A, P, and V represent the swept area of the turbine rotor, power coefficient, air density, power output, and wind speed, respectively.

(b) Wind Speed: The wind speed model captures the variation in the wind speed over time. It can be modeled using stochastic processes or statistical methods based on historical wind speed data. A simplified representation of the wind speed model as follows:

$$V_{wind-Speed} = g(t) \quad (7)$$

where V represents the wind speed and t represents time.

(c) Electric Power Conversion: The electrical power conversion model relates the mechanical power generated by the wind turbine to the electrical power output. This model considers factors such as generator efficiency, losses, and control strategies. A simplified representation of the power conversion model is presented as follows:

$$P_{wind-elec} = \eta_{conv} \times P_{mech} \quad (8)$$

where P_{elec} represents the electrical power output, P_{mech} represents the mechanical power, which is generated by the turbine, and η_{conv} represents the conversion efficiency.

(ii) Solar (P-V) DG Model.
The solar (photovoltaic) DG modeling consists of the following steps:

(a) PV Panel Output Power: The output power of a PV solar panel is typically modeled using the power–voltage (P-V) characteristic curve or current–voltage (I-V) characteristic curve. These curves relate the panel's voltage and current to the generated power and can be represented by equations as follows:

$$P_{solar} = V * I \quad (9)$$

where P is the solar panel output power, I is the solar panel current, and V is the solar panel voltage, obtained from the I-V curve.

(b) Solar Irradiance: The output power of a PV solar is related to the incident solar irradiance, temperature, and other factors. The solar irradiance model represents the variations in solar irradiance (incident solar power per unit area) over time. It can be modeled using historical data, empirical models, or numerical weather prediction models. A simplified representation of the solar irradiance model is as follows:

$$G_{solar} = f(T) \tag{10}$$

$$P_{solar} = g(G, T) \tag{11}$$

where P represents the power output, G represents the solar irradiance, and T represents the temperature.

(c) Temperature Dependency Equation: PV panel performance is affected by temperature variations. The temperature dependency model accounts for the decrease in panel efficiency as the temperature rises. This can be presented as follows:

$$P_{temp.} = f(v) = \mathrm{P}_{ref.} \times [1 + \alpha \times (T - T_{ref})] \tag{12}$$

where P_{temp} is the temperature-adjusted power output, T_{ref} is the reference temperature, P_{ref} is the power output at the T_{ref}, α is the temperature coefficient, and T is the temperature of the actual panel.

2.5. Synchronous and Asynchronous Different Types (I-IV) of DG Mathematical Model

The optimal sizing at various placements for different types of DGs is determined by using the power losses formula as follows. The $P_{(DGi)}$ is the active output power and $Q_{(DGi)}$ is the reactive output power of DG; similarly, $P_{(Di)}$ is the active power demand and $Q_{(Di)}$ is the reactive power demand at the i bus, represented as follows:

$$P_{(i)} = P_{(DGi)} - P_{(Di)} \tag{13}$$

$$Q_{(i)} = Q_{(DGi)} - Q_{(Di)} \tag{14}$$

$$Q_{(DGi)} = \alpha * P_{(DGi)} \tag{15}$$

where assuming $\alpha = \tan(\cos^{-1} PF_{DG})$ and $\mathrm{PF_{DG}}$ is the DG unit power factor. From Equations (14) and (15), the yield of the injected reactive power at the i bus can be represented as follows:

$$Q_{(i)} = \alpha * P_{(DGi)} - Q_{(Di)} \tag{16}$$

By substituting Pi and Qi from Equations (13) and (14) into Equation (15), we obtain a modified power loss equation with respect to its active power and reactive power according to the types of DGs.

(I) Type-1 DG.

In this case, when it only supplies active power $P_{(i)}$, set $\alpha = 0$, and the power factor is considered as unity (PF_{DG} = 1).

$$Active\ Power\ Loss\ Reduction(P_{LR}) = \frac{P_{Loss} - {P_{Loss}}^{DG}}{P_{Loss}} \times 100\% \tag{17}$$

(II) Type-2 DG.

In this case, it supplies both active power $P_{(i)}$ and reactive power $Q_{(i)}$ with $\alpha \neq 0$, α is considered as a constant, and '$\mathrm{PF_{DG}}$' is set to be equal to total combined load values.

$$Rective\ Power\ Loss\ Reduction(Q_{LR}) = \frac{Q_{Loss} - {Q_{Loss}}^{DG}}{Q_{Loss}} \times 100\% \tag{18}$$

(III) Type-3 DG.

In this case, when active power $P_{(i)}$ is supplied and reactive power $Q_{(i)}$ is consumed/absorbed, then consumed reactive power is considered as a function of active power and taken as a partial derivative of the power formula with respect to active power $P_{(i)}$ with zero.

$$Q_{DG(i)} = -(0.5 + 0.04{P_{DG(i)}}^2) \tag{19}$$

(IV) Type-4 DG.

In this case, when it supplies only reactive power $Q_{(i)}$, then take the partial derivative of the power formula with respect to a reactive power $Q_{(i)}$ of zero. This unit is based on a synchronous machine.

$$S_{DG(i)} = \sqrt{{P_{DG(i)}}^2 + {Q_{DG(i)}}^2} \tag{20}$$

2.6. Technical Objective Function

In this section, various objective functions examine the optimal allocation and appropriate capacity of DG units based on single and multiple objectives. The objective functions are mathematically formulated as follows:

(1) Minimization of Power System Loss.

The minimum function with and without DG for the power loss minimization is formulated as follows:

$$PLI = \frac{\sum_{i=1}^{ni} \left(P_{(Loss,i)}\right)^{WithDG}}{\sum_{i=1}^{ni} \left(P_{(Loss,i)}\right)^{WithoutDG}} \tag{21}$$

The first objective function is formulated as follows:

$$f_1(k) = minimize(PLI) \tag{22}$$

where $P_{(Loss,\,i)}$ is the power loss without DG and ${P_{(Loss,\,i)}}^{DG}$ is the power loss with DG and for the kth lines. '*i*' is donated as a branch, and '*ni*' is donated as the total number of lines or branches.

(2) Voltage Deviation.

The power system voltages could be within a definite range due to maintaining the power quality. The minimum function for voltage deviation mathematically can be presented as follows:

$$VD = abs\left(\sum_{i=1}^{Nb} \frac{\left(V_{ref} - \left\{(V_i - V_{min})^2 + (V_i - V_{max})^2\right\}\right)}{V_{ref}}\right) \tag{23}$$

$$\text{where } i = 1, 2, 3, \ldots\ldots, N_b. \tag{24}$$

The second objective function is formulated as:

$$f_2(k) = minimize\left(\sum_{i=1}^{nb} (VD)\right) \tag{25}$$

where '*VD*' is voltage deviation, 'V_{ref}' is reference voltage, 'V_i' is bus voltage, V_{max} represents the maximum, and V_{min} represents the minimum acceptable voltage magnitudes at i^{th} bus, respectively. '*nb*' is donated as the total number of node buses.

(3) Stability Index.

The combined stability factors are used for optimizing the power system by identifying the control variables. The power system voltages and power could be within a definite range for maintaining the power system stability [64].

(a) Voltage Stability Index.

The weakest voltage bus in a power system is identified using the stability index (SI). This index will identify the network's proper weakest link, which may eventually result in voltage stability as the load increases. The index value, known as the voltage stability index, is determined by following Equation (26).

$$VSI(k) = {V_{(i)}}^4 - 4(P_{(k)}R_{(ik)} + Q_{(k)}X_{(ik)}) \times {V_{(i)}}^2 - 4(P_{(k)}X_{(ik)} - Q_{(k)}R_{(ik)}) \quad (26)$$

Total voltage stability improvement (TVSI) is defined to see the effects of DG on all system buses, given by Equation (17).

$$TVSI = \sum_{k=1}^{nb} \frac{\{VSI(k)\}^{WithoutDG}}{\{VSI(k)\}^{WithDG}} \quad (27)$$

where 'V' is the voltage at i^{th} bus, 'P_k' is total power at the k^{th} bus, 'R_{ik}' is the resistance of branch ik, 'X_{ik}' is the reactance of branch ik, 'nb' is the total donated number of buses, and '$VSI(k)$' is donated to the value of voltage stability at the k^{th} bus.

(b) Power Stability Index.

Power stability improvement (PSI) is defined to see the impacts of DG on power stability. Power stability is calculated by using Equation (28):

$$PSI = \sum_{k=1}^{ni} \frac{\{P(k)\}^{WithDG}}{\{P(k)\}^{WithoutDG}} \quad (28)$$

where 'ni' is the total number of donated branches, and '$PSI(k)$' is the value of donated power stability at the k^{th} branch.

(c) Loading Margin and Line Stability Index.

The value of additional electric load, at any specific point in operation that would cause a collapse in voltage, is referred to as the system's loading margin or line stability (L_{mn}). The approach of factor analysis for modal participation is proposed. L_{mn} is presented mathematically as follows:

$$Lmn = \frac{4 * Q_{(k)}}{V_{(i)}\{\text{Sin}(\theta - \delta)\}^4} \leq 1.00 \quad (29)$$

where 'L_{mn}' is the line voltage stability index, 'Vi' is the sending end voltage, 'Q_k' is the receiving end load, 'θ' is the angle of line impedance, and 'δ' is the difference angle between the sending and receiving bus. The value of 'L_{mn}' should be less than unity under stable conditions; when 'L_{mn}' exceeds unity, the system becomes unstable. As a result, the 'VSI' and 'L_{mn}' formulas are in opposition to each other; lower values of 'VSI' indicate bus instability, and greater values of 'L_{mn}' indicate line instability. Line stability improvement (LSI) is defined to see the impact of DG on line stability, as given in below Equation (30):

$$LSI = \sum_{j=1}^{ni} \frac{(Lmn_{(j)})^{WithDG}}{(Lmn_{(j)})^{WithoutDG}} \quad (30)$$

(d) Combined Stability Index.

The combined stability index mathematically can be presented in the following equation:

$$CSI = 0.5 * \left\{ \frac{1}{\max(TVSI(nb))} \right\} + 0.5 * \left\{ \frac{1}{\max(LSI(ni))} \right\} + 0.5 * \min\{PSI(ni)\} \quad (31)$$

where '*CSI*' is the combined stability index of bus and line voltage, '*nb*' is the total number of buses, and '*ni*' is the branches in the network. It can be seen from Equation (31) that the inverse of LSI is taken into account in the CSI formulation since the value of PSI and VSI will be minimized and the value of LSI will be maximized. It should be noted that terms are multiplied by the constant 0.5 in order to create symmetry in the CSI findings. As a result, the value of CSI will be in the range of 0 to 1 to optimize the stability for the selection of candidate buses where DG units are to be installed. The third objective function is formulated as:

$$f_3(k) = minimize(CSI) \quad (32)$$

where '*i*' is donated as a branch, '*ni*' is donated as the total number of lines or branches, '*nb*' is donated as the total number of node buses.

(4) DG Optimal Sizing.

This objective function is used to optimize the DG size for the selection of candidate buses where DG units are to be installed. The optimal size of DG can be formulated by the following fourth function:

$$S_{(DG,i)} = \frac{P_{DG^{(i,j)}}}{\sum_{j=1}^{np} \left\{ P_{Load^{(i,j)}} \right\}} \quad (33)$$

$$f_4(k) = minimize(S_{DG}) \quad (34)$$

where $P_{DG(i,j)}$ is donated as the value of power on the bus for the i^{th} branch, $P_{Load,(j)}$ is donated as the value of active power of the load on the bus for *j* point, '*np*' is donated as the total number of load points. $S_{(DG,i)}$ is donated as the size of DG for i^{th} bus.

2.7. Operational Technical Constraints

In all optimization processes, the following constraints should be considered:

A. Equality Constraints

1. Active Power (P_{Grid}) Balance Equations:

$$P_{Grid} + \sum_{i=1}^{ni} (P_{(DG,i)}) = \sum_{i=1}^{ni} (P_{(d,i)}) + \sum_{j=1}^{nb} (P_{(Tloss,j)}) \quad (35)$$

2. DG Capacity Constraints:

$$\sum_{i=1}^{ni} (P_{(DG,i)}) \leq \frac{3}{4} \times \sum_{i=1}^{ni} (P_{(d,i)}) + \sum_{j=1}^{nb} (P_{(Tloss,j)}) \quad (36)$$

where P_{DG} represents the power generation and P_d represents the power demand.

B. Inequality Constraint

1. Voltage Limit Constraint.
The inequality constraints of voltages as defined below.

$$V_{i.min} \leq V_i \leq V_{i.max,} \quad (37)$$

where *Vi* is donated voltage at the i^{th} bus. For $i = 1, 2, \ldots\ldots, N$, the voltage minimum value is 0.95 per unit (p.u), and the maximum value is 1.1 per unit (p.u).

2. Current Limitations Constraint.

$$I_i \leq I_{rated.max} \tag{38}$$

The 'I_i' is donated as branch current and 'I_{rated}' is rated current limit in the line.

3. DG Units Power Capacity Constraints: The total DG power capacity is restricted and should be within maximum and minimum permissible values for each DG capacity as defined below.

$$P_{DGi\ min} \leq P_{DGi} \leq P_{DGi\ max} \tag{39}$$

4. Power (P_{Loss}) Loss Limits Constraints: The total power loss after placement of DG should be lesser than the power loss before DG was integrated.

$$P_{Loss,i}{}^{DG\ min} \leq P_{Loss,i}{}^{DG} \leq P_{\ Loss,i}{}^{DG\ max} \tag{40}$$

5. The next inequality constraint is the size of DG and the size can be determined by the different types of DG penetration levels, and it can be written as.

$$DG_{size} = \frac{\sum_{i=1}^{n} S_{Total(Load,i)}}{100} * Penetration\_Level \tag{41}$$

$$S_{max} \geq S_{DG} \geq S_{min} \tag{42}$$

So, the size of the DG should be between 25% and 75% of the distribution system's total load.

$$0.25 \times P_{load} \leq P_{DG} \leq 0.75 \times P_{load} \tag{43}$$

6. The 'Power Factor' ($P.F._{DG}$), which is adjusted at a practical value of, i.e., 0.85, is the last but not the least important parameter.

$$|\,P.F._{max}\,| \geq |\,P.F._{DG}\,| \geq |\,P.F._{min}\,| \tag{44}$$

2.8. Proposed Multi-Objective Function for Optimization

This section investigates various objective functions for optimizing the placement and sizing of DGs based on single and multiple objectives. Multiple objective optimization problems (MOPs) are commonly referred to as multi-objective decision-making, multi-criteria optimization, or Pareto optimization [65,66]. These optimization objectives are designed to maximize or minimize multiple objective functions simultaneously. Therefore, multi-objective functions, such as power losses, voltage deviations, and stability factors, are addressed using the following mathematical formulations. The multi-objective problems (MOPs) can be mathematically expressed as follows:

$$MinF(k) = [f_1(k), f_2(k), f_3(k), \ldots\ldots\ldots\ldots, f_n(k)] \tag{45}$$

where *F(k)* is the objective function at the variable *k*'s for the n^{th} objective function which is donated by $F_n(k)$; *K* is called the decision variable, $k = \{K_1, K_2, K_3, \ldots\ldots\ldots, K_n\}$.

The weighted sum approach is a powerful tool, which is used for optimizing power systems by identifying the control variables. The objective function, as formulated in Equation (48), can be combined using the weighted sum approach to create a multi-objective function that balances the various single-objective functions.

$$Minimize(mof) = \min(w_1 f_1 + w_2 f_2, \ldots\ldots\ldots + w_n f_n) \tag{46}$$

where f_1, f_2, f_3, and f_n are objective functions related to power losses, voltage profiles, sizes and stability.

$$\sum_{i=1}^{n} |w_i| = 1$$

where w_1, w_2, and w_n are the weighting factors assigned to each objective function. The effectiveness of the proposed strategy for the sizing and optimal placement of DG will be evaluated using the weighted sum method. In this scenario, the multi-objective function weighted sum is comprised of power losses, voltage profiles, sizes, and stability [67–70].

$$f(t) = w_1 * f_1 + w_2 * f_2 + w_3 * f_3 + w_4 * f_4 \quad (47)$$

To find the optimal combination of weights that satisfies the previously defined multi-objective functions, a weight impact study on fitness values has been conducted for analysis purposes. As a result, the weighting factors for total power losses should range between 0.4 and 0.9, with the remaining percentage allocated to voltage variations. In the proposed method for optimal DG placement and sizing, the MFDO optimization technique is used to determine the fitness function. The overall fitness function, incorporating the power system's technical objectives, is as follows: the objective function focuses on minimizing both power losses and voltage deviations, as shown in Equation (48).

$$F\min = \sum_{i=1}^{N} w_1 * (PLI_{(i)}) + \sum_{i=1}^{N} w_2 * (VD_{(i)}) + \sum_{i=1}^{N} w_3 * (CSI_{(i)}) + \sum_{i=1}^{N} w_4 * (DG_{size(i)}) \quad (48)$$

$$Subjected\ to\ F_{min} = \begin{cases} 0.95 \le V_i \le 1.1 \\ P_{DGi.min} \le P_{DGi} \le P_{DGi.max} \\ V_{DG.min} \le V_{DG} \le V_{DGmin} \\ I_{i*j} \le {I_{i*j}}^{max} \\ P_{DG} \le {P_{DG}}^{max} \\ 0.4 \le w \le 0.9 \\ 0.4P_{load} \le DG_{capacity} \le 0.75P_{load} \end{cases} \quad (49)$$

3. Optimization Techniques

This section provides a brief introduction to recently nature-inspired optimization algorithms, specifically the Fitness-Dependent Optimizer (FDO), the Improved FDO (IFDO), and the proposed Modified Fitness-Dependent Optimizer (MFDO), along with an overview of their actual working mechanism.

3.1. Modified Fitness-Dependent Optimizer (MFDO)

The modified enhanced variant of FDO so-called Modified Fitness-Dependent Optimizer (MFDO) is proposed in this research work. The modified variant of the Fitness-Dependent Optimizer is a recently developed metaheuristic algorithm, introduced by Hozan and Bryar in 2024. This particular newly introduced metaheuristic algorithm is therefore well suited for solving various applications, especially in the context of engineering optimization problems. Although FDO and its variants demonstrate competitive performance, they exhibit several key issues, including premature convergence, poor exploitability, slow convergence, prediction accuracy, high space complexity, insufficient memory, longer execution time, not avoiding local optima, and an inability to refine solutions or effectively solve optimization problems. To address these challenges, we introduce modifications and hybridization to the original FDO. This research work proposed the hybridization and modification of the original FDO to enhance its performance in terms of higher imputation and reducing the computational time while also resolving the issues associated with previous variants of FDO. The proposed MFDO algorithm has greater exploration and exploitation capabilities, it can be readily constrained into local optima, it converges more rapidly, and it performs better than both the original FDO and its improved

variants. Notably, the MFDO demonstrates significant improvements when applied to multiple real-world applications, providing highly competitive results in comparison to FDO and its improved variant.

3.2. Fitness-Dependent Optimizer (FDO)

The Fitness-Dependent Optimizer (FDO) is a recently developed swarm intelligence-based algorithm introduced by Abdullah and Rashid [71]. This particular metaheuristic algorithm has been used by researchers to solve various applications, especially in the context of engineering optimization problems. FDO is a novel optimization technique inspired by the decision-making and reproductive processes of bees swarming. The fitness function generates weights that guide the search agents during the exploitation and exploration phases, allowing for the calculation of the pace of their movements. This algorithm effectively replaces the reproductive mechanisms of swarm bees. A significant aspect of the FDO algorithm is its reliance on hive exploration, which involves selecting suitable options for scout bees. The artificial scout population is randomly initialized at the beginning of the algorithm within the search space defined by $Xi = (i = 1, 2 \ldots\ldots n)$; each scout's position represents a newly identified hive. Similar to how scout bees continue searching for the most suited hive, once they identify a better hive, they ignore the previously found hive. Whenever a new feasible solution is discovered, solutions that are inferior to this new one will be neglected. If the scouts cannot identify a better solution than the one previously found, they will regard the current solution as the best option. In this approach, artificial scouts randomly explore the landscape through a mechanism that combines fitness weights and random walks. Once a decision is made, the remaining scouts return to the hive to establish their new lives as a colony. The FDO employs fitness weight (fw), which is modeled after the collective decision-making process of bees, to guide the search agents toward the optimal solution. Each search agent, or artificial scout bee, can utilize any of the hives to represent a possible solution, with the global optimal being represented by the best hive. The specifications of each hive include its volume, position, and size, which indicate the fitness function of the corresponding solution. The FDO algorithm begins by establishing the upper and lower boundaries to randomly allocate solutions to the scout bee population. The scout bees use a combination of fitness weight mechanisms and random walks to find hives. To change their position, the scout bees adjust their current location by adding a pace value. The movement of the scout bees is calculated as follows:

$$X_{i,t+1} = X_{i,t} + pace \tag{50}$$

where X is donate the scout bee (search agent), t indicate the current iteration of the artificial scout bee that is now in use, i is the search scout bee (search agent), and $pace$ is the scout bee's movement rate and direction. The value of fitness weight (fw) determines the $pace$. Equation (51) is used to determine the fw. The direction of pace is entirely determined by a random system, but the pace is typically determined by fw, or fitness weight. Therefore, the fw of minimization problems can be calculated as:

$$fw = \left| \frac{x^*i, tfitness}{xi, tfitness} \right| - wf \tag{51}$$

where $xi, tfitness$ is the fitness function of the global best solution,$xi, tfitness$ is the fitness function of the current solution, and wf is the weight factor (its value is either 0 or 1). Moreover, fw and $pace$ depend on different cases and the rules are stated as follows (52)–(54):

$$\begin{cases} if\ fw = 1, \quad or \quad fw = 0 \quad or\ x_{i,tfitness} = 0\,, \quad pace = x_{i,t} * r & (52) \\ fw < 1\ and\ fw > 0 \begin{cases} if\ r < 0, \quad pace = fw * (x_{i,t} - x^*{}_{i,t}) * (-1); & (53) \\ if\ r \geq 0, \quad pace = fw * (x_{i,t} - x^*{}_{i,t}) & (54) \end{cases} \end{cases}$$

where the random levy number donates r and its value range is [1, 1]; the levy fight form has been utilized due to its good distribution curve [34].

The weight factor is written as wf, which can only have a value of 0 or 1 and is used to control the fitness weight (fw). The fitness function value of the current best global solution is donated by $x^*i, tfitness$. The fitness function value of the current solution is donated by $xi, tfitness$. A high level of convergence and low possibility of coverage are shown if $wf = 1$. However, if wf is equal to zero ($wf = 0$), it will not affect Equation (51) and can be ignored. If the variable is $wf = 0$, it will provide a more stable search. However, it is actually the reverse because the fitness function's value is the only factor that depends on the optimization problem. However, fw will fall in the range of [0, 1]. However, in certain cases, fw can be equal to 1, such as when the current solution is the global best solution or when the global best solution and the current solution have the same fitness values. Moreover, if $x^*i, tfitness$ = 0, there is a chance when $fw = 0$.

$$fw = 1; if \begin{cases} f(X^*_{i,t}); \ is\ the\ current\ solution \\ f(X_{i,t}) = f(X^*_{i,t}); \ and \qquad (55) \\ f(X_{i,t})\ and\ f(X^*_{i,t})\ boths\ fitness\ value\ are\ same \ (56) \end{cases}$$

Generally, the flow chart of the FDO algorithm is shown in Figure 5, which depicts the algorithm's procedures [71].

(A) Limitations of FDO and Improved variant of FDO.

The FDO algorithm is effective in identifying optimal solutions; however, it has several limitations. The main drawbacks include slow convergence, and unbalanced exploration and exploitation. Therefore, the existence of numerous randomized parameters such as wf, pace, fw, updating equation, levy flight, places limits, and optimum updating solution in FDO. Hence, in FDO, the setting of wf depends on convergence; if this value is zero, it adversely affects convergence performance, leading to low convergence, as stated in the paper [71]. Another issue with the FDO is its unbalanced exploration and exploitation. Because it relies on wf, current fitness, and fitness of the best agent, it struggles to achieve a proper balance between these two phases. Furthermore, the use of a randomization-based pace exacerbates this imbalance. The poor performance of the FDO can also be attributed to the aging of its solutions, which arises from applying pace equations that yield suboptimal results and using a fixed value for wf. According to literature-based research, FDO performs inadequately compared to various other algorithms, as it exhibits insufficient exploitation capability and imbalance issues between the exploration and exploitation phases [71].

An improved version of the Fitness-Dependent Optimizer (FDO), referred to as the Improved Fitness-Dependent Optimizer (IFDO), was developed by Daniel et al. in 2019 [72]. The IFDO is more effective in finding the optimal solution. The IFDO was developed to overcome the certain drawbacks of FDO, enhancing its performance and achieving faster convergence. However, like other algorithms, the IFDO has its own limitations. Key drawbacks include premature convergence and poor exploitation capabilities. Additionally, the IFDO has more complexity, and it takes more computational time for large datasets. It tends to prematurely converge to local optima, especially in complex search spaces and faces scalability issues that can degrade performance. The IFDO also requires more computational resources and memory space and may necessitate tuning for specific problems, making it difficult to identify the optimal parameter set. Furthermore, it struggles to accurately avoid local optima and refine solutions. Therefore, modifications or a hybridization approach are necessary to mitigate the issues associated with the FDO and to achieve faster convergence along with a higher quality of optimal solutions.

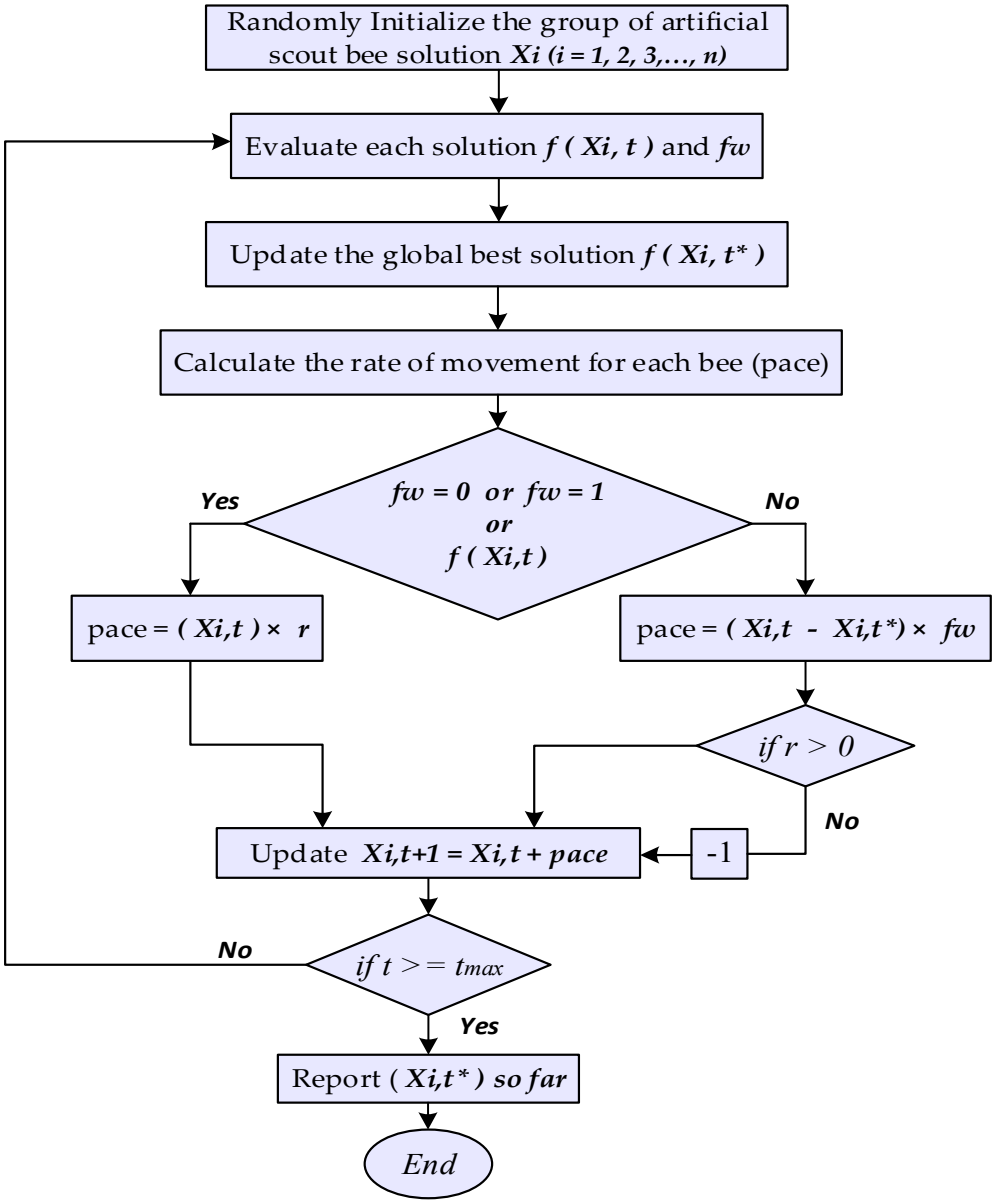

Figure 5. The FDO algorithm's flow chart.

3.3. Modifications in FDO

The Fitness-Dependent Optimizer (FDO) was improved for the first time in 2019 by Daniel et al. to overcome their drawbacks [72]. While both the FDO and its improved variant perform competitively, they exhibit several key issues, including premature convergence, low exploitation, slow convergence rate, poor exploitability, prediction accuracy, and difficulties in avoiding local optima and refining solutions. Therefore, the modification is suggested as a solution for FDO and its variant issues to enhance their performance. Consequently, a modification is proposed with the concept of hybridization and modifying the parameter strategy, which is introduced in the FDO to enhance their performance. This paper proposes the modification in FDO based on three methods. First, the pace equation is optimized by incorporating a lambda (λ) parameter in the FDO pace equation. Second, the weight factor range is refined to optimize it between 0 and 0.2 [0, 0.2], which is utilized to determine fitness weight. Third, parameters from the sine–cosine algorithm are hybridized; this includes updating fitness weight and pace, which relate to the bees' speed using the sine cardinal mathematical function. This paper proposes a hybrid modified variant of the FDO, known as the Modified Fitness-Dependent Optimizer (MFDO), which integrates

using optimized pace, weight factor, and sine–cosine parameters, and indicates that the MFDO demonstrates outstanding performance compared to other optimization algorithms. Ultimately, the MFDO proves to be an efficient solution for various optimization problems.

A. Enhanced FDO using Optimized Pace Equation.

In the FDO, the pace parameter is utilized to guide both the direction and magnitude of the artificial bees' movement. This paper proposes a modification to the FDO by incorporating the lambda (λ) parameter into the pace equation, as shown in Equation (57). The value of lambda is set to 0.1, which requires minimal computation time to achieve the optimal solution. Consequently, this adjustment reduces the overall computation time and enhances the performance of the algorithm.

$$X_i^{t+1} = X_i^t + pace + Lambda \tag{57}$$

where '*i*' is the current artificial scout bee (search agent) and (*t*) is the current iteration; the pace is the movement rate and artificial bee direction; *X* is the artificial bee.

B. Enhanced FDO using Optimized Weight Factor and Global Fitness Weight.

This work presents the Modified Fitness-Dependent Optimization (MFDO) algorithm, which is an enhancement of the original FDO. In the MFDO, an optimized weight factor is incorporated to regulate the fitness function value during the exploration and exploitation phases. By integrating this optimized weight factor and global fitness weight into the search process, the proposed algorithm's performance can be significantly improved, leading to enhanced convergence and solution quality.

In the optimization technique, randomizations can play a major role in exploration and exploitation. Therefore, there are numerous methods for producing random numbers. Consequently, FDO has several randomly generated areas, including fw, wf, and the levy flying mechanism. FDO initially used 0 for weight, and it can use the value of wf either 0 or 1 [71]. On the other hand, the IFDO generates a weight factor (wf) in the range of [0, 1] [72]. The proposed modified enhanced variant of FDO is introduced in this work, which is based on the original FDO and IFDO. The MFDO algorithm consists of the weight factor (wf) randomization. In MFDO, the weight factor (wf) is used in the [0, 0.2] range, which is randomly assigned. Moreover, the fitness weight was controlled by a weight factor (wf) in the IFDO. Nevertheless, in the majority of cases, the wf was neglected [71,72]. However, in MFDO, the weight factor (wf) is used whenever a better fitness weight is obtained. But any time a higher fitness weight is achieved using the optimized weight factor (wf) in MFDO, the algorithm achieves earlier convergence toward global optimality. It is appropriate to cover the search space to take into consideration that the MFDO algorithm is enhanced by updating every scout in each iteration. Pace is used in the original FDO, both for the artificial bee's direction and degree of movement, to control the pace using the regular fitness weight (fw) value. However, the pace direction is entirely determined by random mechanisms. Therefore, Equation (51) expresses the minimizing of fw. When using random phenomena to control the fitness weight (fw) instead of the original FDO, where the weight factor is assumed to be 0 or 1, the weight factor in FDO is typically set to 0. According to the development of the FDO algorithm, the weight factor is used to control the fitness weight and has two possible values: 0 and 1. When the wf = 0, it indicates a more stable search, and when the wf = 1, it indicates high convergence and low coverage possibility. The IFDO regulates the fitness weight by producing a weight factor in the range [0, 1]. However, this work pointed out that although the value of the fitness function is dependent on the optimization problem, the reverse may also occur. Therefore, in order to improve the FDO performance, we employ a random technique in our enhanced Fitness-Dependent Optimizer to regulate the fitness weight by producing a weight factor in the range [0, 0.2]. The MFDO algorithm generates a weight factor (wf) in the range of [0, 0.2], as demonstrated in Equation (58), which illustrates how we change Equation (51)

in our proposed modification. The improvement of the FDO algorithm in terms of fitness weight can be expressed as follows:

$$fw = \left| \frac{x^*_{i,tfitness}}{x_{i,tfitness}} \right| \tag{58}$$

Equation (58) is used to determine the fitness weight value. In contrast to the preceding equation, the weight factor in Equation (58) can be neglected if the value of fitness weight (fw) is equal to or less than the generated weight factor (wf). If the value is less than or equal to the generated weight factor, as indicated in the MFDO procedure (refer to Figure 6), the weight factor is neglected if determining the fitness weight. If not, then control the fitness weight by involving the weight component using Equation (59).

$$fw = fw - wf \tag{59}$$

As can be seen from Equation (51), this mechanism in the FDO tends to result in slow convergence. Thus, FDO improved the fw by calculating a weight factor value in the range [0, 0.2] by using a random mechanism. Furthermore, fw is calculated in Equation (59) if one of these conditions is true: $xitfitness = 0$, $fw = 0$, so, $fw > wf$. Otherwise, fw is calculated based on Equation (58).

This is a new method of determining the fitness weight, which is typically avoided by ignoring *wf*, and in many circumstances, *wf* participates reasonably. According to the MFDO, each scout's weight factor is randomly assigned at the beginning of each iteration, and when a new and improved solution is approved, a new *wf* is generated in the new [0, 0.2] range. Next, a new *wf* limited in [0, 0.2] is preferable. In the meantime, the new solution's MFDO will be more stable and have better coverage than the previous one since *wf* is reduced with each iteration and it has more convergence than the setting where *wf* = 0.

Furthermore, whenever a better solution is achieved, in order to maximize the chance of finding the best solution the optimal solution in the shortest amount of time, a new *wf* is created in a new range. Following the addition of the three different conditions to fw, the following conditions are used to determine this parameter.

$$\begin{cases} nfw_t = fw_t - wf_t; & if\ fw_t > wf_t, \quad (60) \\ nfw_t = fw_t; & if\ fw_t < wf_t, \quad (61) \end{cases}$$

where fw_t represents the current fitness weight, and nfw_t is the new fitness weight at the tth iteration represented in Equations (60) and (61). wf_t represents the current weight factor in the range [0, 1]. The wf value decreased from wf to zero during increasing iterations.

Therefore, to further optimize and tune random fw by another type of parameter known as global fitness weight (fw^*) which is used for the best solution found so far by any scout bee over all the iterations. The global fitness weight is represented by fw^*, which is used to refine and donate as in the following Equation (62).

$$wf_t = wf_{t-1} \times r_0; \quad if\ fw^* < fw_t \tag{62}$$

where r_0 is the random number in the range of [0, 1] and wf_t is the current weight factor whose range falls in the [0,wf_{t-1}].

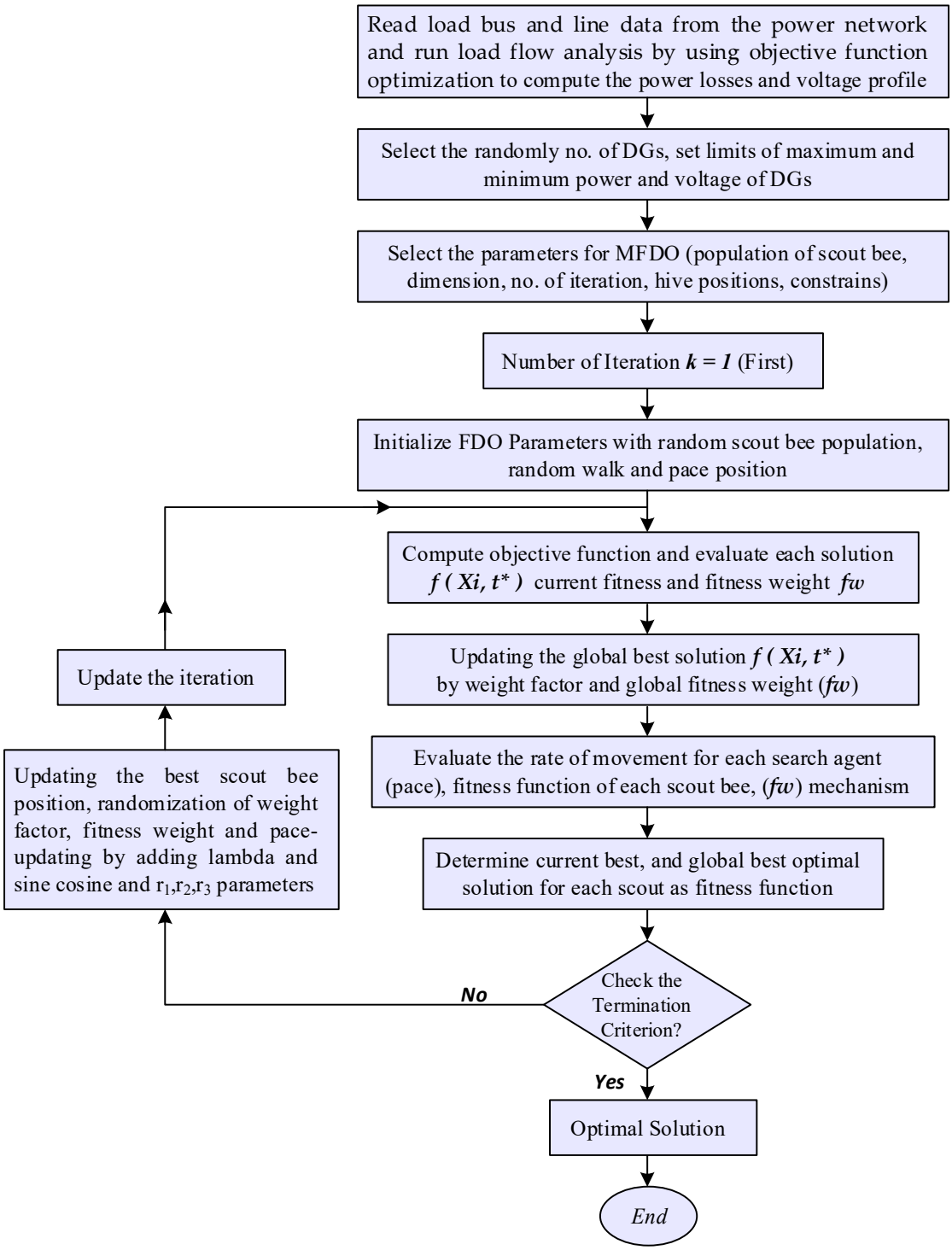

Figure 6. Flow chart for proposed algorithm.

C. Enhanced FDO using Hybridization of Sine–Cosine Parameters.

The FDO exhibits an inevitable slow convergence rate when utilizing the fitness weight (fw) mechanism. The pace-updating strategy described in Equations (52)–(54) may enhance solution diversity, making it more difficult to find the global optimal solution because of the FDO's strong exploration ability. To address this issue, the concept of hybridization and modification of various strategies, specifically pace-updating, global fitness weight, random weight factors, best solution tracking, and conversion parameter strategy, is introduced into the original FDO to improve its performance. This enhancement aims to mitigate

premature convergence, achieve a better balance between exploitation and exploration, and accelerate the convergence rate.

In this work, the hybridization of FDO with the Sine–Cosine Algorithm (SCA) is proposed for solving optimization problems [73]. The SCA, an optimization algorithm introduced by Mirjalili, is known for its effectiveness in solving optimization problems and exhibits high search space exploitation.

This work demonstrates that SCA has high search space exploitation and is based on a population algorithm which was introduced by Mirjalili [74]. The resulting hybrid SC-FDO integrates the sine–cosine scheme into the modified pace-updating mechanism of the original FDO algorithm. Initially, the modified pace-updating mechanism facilitates the search process by exploring several promising solutions in prominent regions. Moreover, it guides the search agents to maintain a balance between exploration and exploitation through this modified approach. The following equations outline the calculation of the modified pace-updating mechanism. The following equations are used to calculate the modified pace-updating equation.

$$\begin{cases} if\ fw = 1, \quad pace = x_{i,t} \times r & (63) \\ if\ fw = 0, \quad pace = r * (x_{i,t} + r_1 * \cos(r_2) * (r_3 * {x_{i,t}}^* - x_{i,t})) & (64) \\ if\ 1 < fw < 0 & \\ \begin{cases} if\ r < 0, \quad pace = fw * (x_{i,t} + r_1 * \sin(r_2) * (r_3 * {x_{i,t}}^* - x_{i,t})) - 1; & (65) \\ if\ r \geq 0, \quad pace = fw * (x_{i,t} + r_1 * \sin(r_2) * (r_3 * {x_{i,t}}^* - x_{i,t})); & (66) \end{cases} \end{cases}$$

where 'r' represents a levy random number within the interval [−1, 1] and r_1, r_2, r_3 are represented by random variables,${x^*}_{i,t}$ is the global best solution, $x_{i,t}$ is the current best solution, fw is the fitness weight, and the weight factor wf is within the [0, 0.2] range. Although the random walk can be implemented in a variety of ways, levy fight has been selected because of its good distribution curve, which results in more steady movements [74,75]. If the fitness values of the global best and current solutions are the same, then pace is calculated as expressed in Equation (63). The $r_1 * cos(r2)$ or $r_1 * sin(r_2)$ are used to guide the scout bees towards exploration or exploitation and can be calculated as Equations (64)–(66). If the values of $r_1 * sin(r_2)$ or $r_1 * cos(r_2)$ are in the [1, 1] range, the scout bees exploit the search solution. However, if the values of $sin(r_2)$ or $cos(r_2)$ are greater than 1 or less than −1, the scout bees explore the diversity of solutions. If ${x^*}_{i,t} - x_{i,t}$, the pace is calculated. Therefore, the pace can be calculated when fw is equal to 1. Consequently, if $fw > 0$, $fw < 1$, and r is less than zero, the pace is calculated. Thus, the pace is found if $fw < 1$, $fw > 0$, and r is greater than or equal to zero. The scout bees can achieve a proper balance between the exploitation and exploration phase by modifying the pace equation mechanism. Thus, r_1 is calculated according to represented Equation (67).

$$r_1 = a^* \times \left(1 - \frac{t}{t\max}\right) \tag{67}$$

where a constant, t, is donated as the current iteration and $t_{\max}$ represents the maximum iteration (it is a constant variable). Furthermore, r_2 represents the movement direction [0, 2π], and r_3 parameter shows the random weight [0, 2]. The scout bee's movement is defined by Equation (68).

$$distance_{best_{bee}} = {r_3}^* \times {x^*}_{i,t} - x_{i,t} \tag{68}$$

The impacts of sine, cosine, and the parameters are presented in Equations (52)–(54). If the value of r_1 is greater than 1, the solutions allow the search agents to investigate the spaces outside of their respective destinations. Meanwhile, if the value of r_1 is smaller than 1, the sine and cosine functions allow a solution to be shifted relative to another solution by exploiting the advantages of the neighboring space. Therefore, in order to improve the scout bees' exploration and exploitation balancing, the conversion parameter strategy is used. The proposed algorithm has improved performance in terms of convergence and

local optima. Therefore, the *sinc* method is used in the original FDO Equation (51) to improve the fw parameter, and the new equation is implemented, which can be expressed in Equation (69).

$$fw = \left| \frac{x^*_{i,tfitness}}{x_{i,tfitness}} \right| \times sinc(\pi * wf) \tag{69}$$

The mathematics *sinc* function which is the contraction "sine cardinal" is represented by $sinc(x)$. There are two conditions that follow as denoted in Equation (70) [74,75].

$$sinc(x) = \begin{cases} 1\,, & if\ \ x = 0 \\ \frac{\sin(x)}{x}\,, & otherwise \end{cases} \tag{70}$$

Moreover, the improved pace updating mechanism of the MFDO is expressed in Equation (71).

$$pace = \begin{cases} x^*_{i,t} \times r \times sinc(\pi * wf)\ ; & if\ fw = 0 \\ distance_{best_{bee}} \times r \times sinc(\pi * wf)\ ; & if\ fw = 1 \end{cases} \tag{71}$$

However, pace is calculated by multiplying $distance_{best_{bee}}$, $sinc(\pi * wf)$ and r ($\pi = 3.1415$ approximately). In conclusion, this work presents the modified pace-updating equation, with the parameter conversion, the global fitness weight parameter ($fw*$) and random weight factor (wf), and the optimal solution-updating strategy in the proposed hybrid FDO method. The efficiency of the hybrid MFDO is enhanced by leveraging the strengths of the Sine–Cosine Algorithm (SCA) to explore refined search areas for optimal solutions. As a result, the hybrid MFDO requires less time to achieve superior outcomes. The exploitation capability and neighboring search of the hybrid MFDO have improved due to the incorporation of SCA features [74,75]. Consequently, in terms of exploring solutions within the search space, the hybrid MFDO demonstrates better performance compared to both the FDO and IFDO algorithms. Furthermore, the hybrid MFDO is evaluated against other algorithms, including FDO, Hybrid GAIPSO, IPSO, PSO, and GA. The findings indicate that the MFDO exhibits a faster convergence rate than the FDO, particularly in selecting the positions of scout bees and avoiding local optima, among other factors [76].

3.4. The Proposed Method

This work optimizes modern energy sources with integrated hybrid power distribution systems with the proposed MFDO method to improve the overall efficiency of the proposed system by minimizing power losses and improving voltage profile and thus stability. The proposed method is based on multi-objective functions and, therefore, is the best solution for solving power system optimization problems. The proposed method is based on the new swarm metaheuristic optimization methodology, which is used to solve multi-objective optimization problems. The proposed algorithm is also known as multi-objective MFDO, which is a hybrid technique that combines the benefits of "modified Fitness-Dependent Optimizer" and "multi-objective optimization".

$$\mathrm{SD} = [\mathrm{SD}_1, \mathrm{SD}_2, \ldots\ldots, \mathrm{SD}_\mathrm{N}] \tag{72}$$

where search space dimension (SD) is defined for D: 1, 2, 3,. . . . . .,N. The MFDO can be implemented once the search spaces and the number of dimensions for each space are specified. The SD is responsible for selecting the optimal position from various positional dimensions, ranging from SD_1 to SD_N. The MFDO is used for optimization problems and is formulated as a multi-objective function with the goals of minimizing power losses, improving voltage profiles, and enhancing stability. The decision variables include power losses, voltage profile, locations and sizes of DG units, and stability. By employing MFDO, optimization can be achieved while considering multiple conflicting objectives. The MFDO incorporates additional mechanisms that enhance the algorithm's "exploitation" and "ex-

ploration" capabilities, resulting in improved convergence times and solution quality. There are several modifications applied to the original FDO algorithm to create the MFDO, such as weight adjustment, neighborhood topology, scout bee position and sizes for hives, scout bee population and rate of movement (pace), fitness weight of scout bee and weight factor, etc. These enhancements have enabled MFDO to achieve better convergence and solution quality compared to the original FDO algorithm, converging more quickly and demonstrating superior performance in locating global optima, particularly in high-dimensional search spaces. The MFDO is a better variant of the classic Fitness-Dependent Optimizer (FDO) algorithm. It enhances the performance, outcomes, and solution quality of the original algorithm by modifying several of its components. One of the key advantages of the proposed method is its ability to provide consistent responses with minimal variance. Additionally, it allows for rapid selection by reducing the number of iterations required. In this context, the output of the multi-objective optimization algorithm is utilized by the MFDO as the initial scout population set, leading to faster convergence. Furthermore, the hybridization of the Sine–Cosine Algorithm and the optimized weight factor method significantly boosts the performance of the proposed algorithm in terms of convergence speed, reduced computational time, and enhanced exploration and exploitation capabilities. This improvement results in a higher quality of solutions, demonstrating the effectiveness of the proposed approach. The proposed method integrates optimal power load flow with the MFDO algorithm and incorporates optimized multi-objective functions, including power losses and voltage stability factors. Optimal optimization is executed using this algorithm, which has been implemented in MATLAB for determining the optimal sizing and location of distributed generation (DG) units. The flowchart depicted in Figure 6 illustrates the procedures of the proposed algorithm.

3.5. The Proposed Algorithm Procedure

The proposed algorithm MFDO procedure consists of the following steps:

Step 1: (Initialization of Population).

A random set of artificial scout bees in the search space X_i $(i = 1, 2, \ldots\ldots\ldots n)$ consists of the initializing population. A solution is represented by each scout bee position. In an attempt to find a better hive, these bees randomly search a larger number of positions and evaluate each one before allocating resources to the best one. The number of scout bees is proportional to the size of the population, and each one is equipped with parameters (P_{Loss}, V_D, SI, and DG_{size}) that indicate the power quality and stability of the power network. In this scenario, every scout represents a possible solution and is randomly investigating more positions in an attempt to find a better hive.

Step 2: (Fitness Weight of Scout Bee and Balance of Randomization).

The fitness weight is used to evaluate each scout bee position. The scout bees are searching randomly for a better hive.

The previous position is abandoned when a better position is discovered. Thus, the algorithm finds a new optimum solution at each position. However, it will revert to its previous solution in search of the optimum solution if the present forward direction is unable to produce an optimal solution. The fitness weight is used to determine the fitness weight value; it can be expressed as follows:

$$fw = \left| \frac{x^*i, tfitness}{xi, tfitness} \right| - wf \tag{73}$$

In order to improve the FDO the balance randomization of the wf is employed for every scout in each iteration. It is used to determine the fitness weight value. It can be neglected if the value of fitness weight (fw) is equal to or less than the generated weight factor (wf).

$$fw = fw - wf \tag{74}$$

Step 3: (Movement of Scout Bee and Updating Position Mechanism).

Scout bees add *pace* to their current position and show their moment as they search for the best solution. The scout bee moves from its current position to the next position by adding *pace* (p) in order to find a better position, as illustrated in Equation (75).

$$X_i^{t+1} = X_i^t + pace \tag{75}$$

The updating pace is proposed using lambda (λ) added in the pace equation. The value of lambda is 0.1. The position of the scout bee is updated using the lambda, as illustrated in Equation (76).

$$X_i^{t+1} = X_i^t + pace + Lambda \tag{76}$$

Step 4: (Modification and Hybridization).

The concept of hybridization with sine–cosine parameters and modified pace-updating, global fitness weight, random weight factor, best solution, and conversion parameter strategy are introduced in the FDO to enhance their performance.

Step 5: (Stoppage/Termination Criteria).

The positions of the new hives are updated and the fitness value of each scout bee is calculated for every iteration. Until a termination condition is met, that is, until the maximum number of iterations $MaxIt$ or $tmax$, this procedure is repeated. The global best solution is generated as the ultimate solution of iterations at the conclusion.

3.6. The Proposed Algorithm Parameter Settings and Convergence Criteria

The algorithm parameters such as population size, dimension, position, maximum iterations, search space boundaries, and fitness function are configured based on the problem. The specific parameters setting and convergence criteria are required to effectively find optimal solutions.

1. Population Size (N): The number of individuals or number of agents (solutions) in the population. A larger population can explore the search space more thoroughly but requires more computational resources. The typical value ranges from 20 to 100 (depending on the problem's complexity and dimensionality).
2. Maximum Number of Iterations (MaxIter): The maximum number of iterations or generations for which the algorithm will run before stopping. The typical value ranges from 100 to 1000 (depending on the problem).
3. Search Space Bounds: Set upper and lower bounds for each dimension of the search space to ensure agents remain within feasible regions.
4. Fitness Evaluation: Evaluate the fitness of each candidate by using an objective function. They evaluate the fitness of the population. Also, it needs to be maximized and minimized.

$$fitness = evaluateFitness(population, fitnessFunction) \tag{77}$$

5. Movement Update Mechanism: The movement of the variables/individuals is influenced by their fitness function and the updated position of the individual current best fitness and random factor. Update the position of each agent/candidate solution based on objective function fitness.

$$NewPosition = CurrentPosition + \alpha \times (BestPosition - CurrentPosition) \times Rand(Size) \tag{78}$$

The various parameters involve and update the movement.

- Step Size (α): The magnitude of movement controlled by alpha. It can be varying or constant with iteration. The step size decreases over time to find the optimal solution.

- Randomness Factor (β): The stochastic behavior introduces in movement by β, which is allowing search space exploration.

$$X_{i,t+1} = X_{i,t} + \alpha(F(X^t_{best}) - F(X_{i,t})).\beta(rand() - 0.5) \quad (79)$$

where X^t_i is donated as the current position and X^t_{best} is the best position, and $rand()$ is donated as a random number which range is [0, 1].

6. Convergence Criteria: Each scout bee's fitness value is determined until a termination requirement is met or a solution is found. If $t \geq T$ or other criteria are met, then stop the algorithm. If $t \geq T$ or other criteria are met, then stop the algorithm. This can be evaluated by the difference between the current and the optimal solution, as presented in Equation (80).

$$\left| f(x_{i,t}) - f^t_{optimal} \right| < \varepsilon \quad (80)$$

Convergence Rate: It is evaluated by the difference between values of the objective function at t and $t-1$ iterations, as presented in Equation (81).

$$|f(x_{i,t}) - f(x_{i,t-1})| \quad (81)$$

where $f(x_t)$ is donated as the objective function at t iteration, $f^t_{optimal}$ is donated as the optimal objective function, and ε is the tolerance level.

Adjust these settings and criteria to suit your specific problem and ensure that the proposed MFDO algorithm converges effectively to a high-quality solution. The parameter setting adjustment or tuning can help to achieve the best solution.

3.7. Steps for Implementation of the Proposed Algorithm

In this section, we describe the steps for implementation of the proposed algorithm to solve the optimal placement of DG and its sizes in a power-distributed system. The proposed algorithm runs through all iterations. All possible iterations are specified by the user, and this algorithm takes into consideration both the bus voltages and the power losses. It stores the node voltages, total power losses, and size and location pattern of DG for iteration with all buses.

Steps:

- Define the problem: In this step, the objective functions, decision variables, and constraints of the problems are defined. The algorithm parameters are dimension, number of iterations, and population size. The input parameters are system data, load data, line data, number of buses, random DG sizes and locations, power factor, and bus voltage limits.
- Run the load flow analysis and find power losses.
- Run the MFDO algorithm by taking the fitness function.
- Set the control parameter of MFDO.
- Initialize the population: Generate an initial set of the population consisting of random individuals (artificial scout bee) in the search space $X_i(i = 1, 2, \ldots\ldots, n)$. The number of scout bees is proportional to the size of the population, and each one is equipped with parameters (P_{Loss}, VD, SI, DG_{size}) that indicate the power network efficacy and stability.
- A solution is represented by each scout bee position. In this scenario, every scout represents a possible solution and is randomly investigating more positions in an attempt to find a better hive.
- Evaluate the movement of scout bees: Scout bees add $pace(p)$ to their current position and show their moment as they search for the best solution. The scout bees relocate from their current position at iteration 't' to a new position by adding "pace" to find a better position from Equation (50).

- Evaluate the fitness: Evaluate the fitness weight (fw) of the scout bee by calculating the objective function values. A fitness weight (fw) is used to determine the pace. However, the pace's momentum is entirely random. The fw can be calculated from Equation (51). The function weight (fw) should fall between 0 and 1. When the values of ${X^*}_{i,t,f}$, and $X_{i,t,f}$ are the same, then the value of fw will be 1. When ${X^*}_{i,t,f} = 0$, then the value of fw will be 0. Applying the rules can help you avoid $X_{i,t,f} = 0$. The operations outlined involve determining the optimal search agent globally, using Equation (51) to find fw, and applying criteria from Equations (52)–(54) to compute *pace*.
- If optimizing requirements are not fulfilled, then go to the next steps.
- When the new search agent is found, determine a new search agent position, and the algorithm always checks whether the new result (cost function) dominates the old result or not. If it is, the new position will be acknowledged and the *pace* will be kept for possible future use. If it is not, on the other hand, the previously saved *pace* will be utilized in place of the new one in the hopes of producing a better result unless the search agent keeps the current position. The solution's compatibility with the archive will then be determined. It will see the application of the parameter updating to obtain further variant solutions. After updating, the parameters then verify whether or not the solution fits inside the archive. Modification indices are continuously updated by changes to the search environment.
- Update the global best solution by 'weight factor' and 'global fitness weight' using the updated weight factor equation.
- Update the pace equation and each scout bee position using the updated scout bee equation and lambda parameter.
- Evaluate the scout bee and fitness using the objective function and update the "current best" and "global best" if a better solution is found.
- Update the "current best" scout bee and fitness for each scout (if the fitness value is better than the previous best value).
- Update the "global best" and fitness (if a scout bee with a better fitness than the "present global best" is found).
- Apply additional mechanisms such as weight factor adjustment, neighborhood topology, hives, a scout bee, sine–cosine, and r_1, r_2, r_3 parameters, etc.
- Update the "pace" and fitness weight using the update Equations (61)–(64).
- Update the global best solution and global fitness weight fw*.
- Calculate the pace and fitness weight.
- Move accepted and saved.
- Termination criterion: The positions of the new hives and scout bee are updated and the fitness function value of each scout bee is calculated until a stopping requirement is met or the best solution is found (i.e., convergence rate, maximum no. of iterations or $tmax$, are reached or the solution is good enough)
- Return the best solution found.

The proposed MFDO algorithm converges faster and better performance in terms of finding global optima, particularly in high search spaces dimensional as compared to the standard and improved version of FDO and other algorithms. This flow chart outlines the basic steps of a proposed algorithm, which involves initializing the scout bee, updating the hives and pace, evaluating each scout's fitness, and updating the "current best" and "global best" positions. The MFDO also involves additional mechanisms that enhance "exploration" and "exploitation" search space capabilities. The algorithm continues to update the positions of the new hives and the fitness value of each scout bee until a termination criterion is met and returns a set of "Pareto-optimal solutions".

3.8. Advantages of the Proposed Method

The proposed method has numerous advantages over the previously well-known method and avoids the previous conventional methods (i.e., analytical-based method,

second-order method, gradient and iterative method, and heuristic method, etc.) problems such as premature convergence, degradation of searching performance, low processing time, falling into local optimum under complex objective function the high memory consumption and high computational complexity. The proposed method enhances the capability of metaheuristic algorithms (due to hybridization and modification which directly affects the optimization results) so that this innovative approach contributes to increasing the efficiency and robustness of problem-solving strategies. It provides better optimization results for complex and large optimization problems. It has minimum parameters, which makes it faster, simpler, and less complex. It also has a fast convergence rate, and dynamics and can solve nonlinear problems. The existing conventional methods have faced some limitations as discussed in the above section, i.e., computational complexity, accuracy and efficiency, stability, low convergence speed, etc.

The proposed method is used to optimize the search process. It has an adaptive mechanism that adjusts the search behavior based on fitness values. This means the better fitness solution has more influence by significantly on the search process. The proposed method has the minimum parameters that make it faster and easily customized for specific problem types and implementation. The method has collective behavior, which means the multiple particles/agents can work together to find a better solution. The proposed method is a hybrid approach that can better handle multi-objective functions for large and more complex problems and multi-modal or noisy optimization landscapes as compared to existing methods. It also can handle high dimensional and various types of optimization problems. The method allows it to adopt the many optimization problems without adjustment or tuning and can reach high-quality solutions, but conventional methods may require specific problem adjustment, modification, or tuning to obtain the optimal solution. It has a unique mechanism that makes it easier to find a better solution effectively. The proposed algorithm's effectiveness is checked by comparing it with various other algorithms including FDO, Hybrid GAIPSO, IPSO, PSO, and GA. As a result, the proposed method's overall performance is high.

4. Research Results

In this section, the standard IEEE 14-bus and 30-bus benchmark test systems are utilized to integrate different types of DG units. This integration is performed to implement and analyze the proposed method, thereby assessing its validity and effectiveness.

4.1. Case 1: Simulation Results for Case Study IEEE 14-Bus System

The 14-bus test system comprises 14 buses, 13 sectionalizing branches, a nominal system voltage of 11 kV, a total active load of approximately 259 MW, and a total reactive nature connected load of about 73.5 MVAR. Therefore, the power losses of the power network before DG installation have been considered to be 13.551 MW, providing a basis for further analysis and comparison with other scenarios. The load flow analysis results without the integration of DG serve as the base case for the 14-bus system and are presented in Tables 1 and 2, as well as Figures 7 and 8.

Table 1. Results of load flow for a 14-bus system without integration of DG.

Bus Node No.	Voltage Magnitude (p.u.)	Phase Angle Degree	Connected Load		Generation Capacity		Injected Reactive Power (MVar)
			MW	MVar	MW	MVar	
1	1.06	0	0	0	232.481	−15.539	0
2	1.045	−4.987	21.7	12.7	40	46.853	0
3	1.014	−12.742	94.2	19	0	27.106	0
4	1.001	−10.256	47.8	−3.9	0	0	0
5	1.017	−8.765	7.6	1.6	0	0	0
6	1.07	−14.418	11.2	7.5	0	21.545	0

Table 1. *Cont.*

Bus Node No.	Voltage Magnitude (p.u.)	Phase Angle Degree	Connected Load		Generation Capacity		Injected Reactive Power (MVar)
			MW	MVar	MW	MVar	
7	1.05	−13.252	0	0	0	0	0
8	1.080	−13.252	0	0	0	24.51	0
9	1.034	−14.832	29.5	16.6	0	0	0
10	1.033	−15.041	9	5.8	0	0	0
11	1.047	−14.848	3.5	1.8	0	0	0
12	1.054	−15.268	6.1	1.6	0	0	0
13	1.047	−15.308	13.5	5.8	0	0	0
14	1.021	−16.065	14.9	5	0	0	0
Total			259	73.5	272.481	104.477	0

Table 2. Summary of load flow results for a 14-bus system.

Power Loss (MW)	Max Line Loss (MW)	Max Bus Voltage (p.u.)	Min Bus Voltage (p.u.)	Voltage Deviation VD%
13.551	4.306	1.080	1.001	4.16

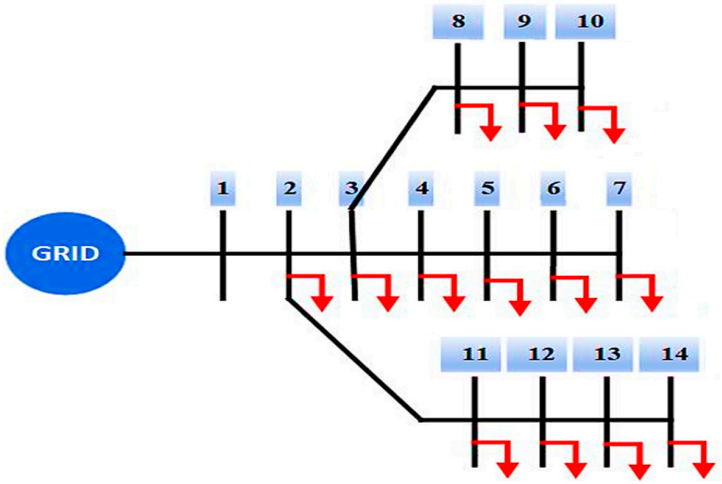

Figure 7. Energy management evaluation on a 14-bus subsystem modeled from a IEEE standard 14-bus framework.

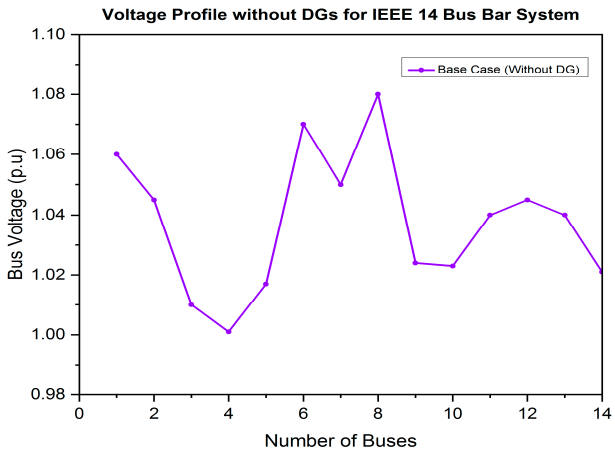

Figure 8. Voltage profile without DG for the IEEE 14-bus system.

Scenario I: Considering Type-1 DG

In this case, the DG is only capable of injecting the active power into a power system. Therefore, different candidate buses are selected to determine the optimal placement of these DG units based on their fitness values. The proposed MFDO method is employed to identify the best allocation of the DG units, providing suitable locations and corresponding sizes for type-1 DG units, as determined by the fitness function. The locations with the lowest fitness values also indicate the most appropriate DG sizes. The backward–forward sweep power flow method is then applied to calculate the associated power losses and voltage levels for different DG sizes and locations. The results obtained are compared with those derived from conventional methods for validation purposes.

It is clear that from Figure 9a, the proposed MFDO method for type-1 DG achieves a greater reduction in power losses compared to conventional FDO methods. While the conventional FDO method reduces losses by 50.94%, the proposed MFDO method achieves a reduction of 50.99%. These results demonstrate the superior performance of the MFDO method over conventional approaches. The MFDO technique proves to be more effective than the FDO technique in determining the optimal placement and sizing of DG units within the power system, specifically for type-1 DG. Figure 9a also illustrates the overall power losses after DG integration. When a DG unit of 11.89 MW is placed at bus 2, the power losses reach their lowest level. The active power losses are reduced from 13.599 MW to 6.641 MW with the incorporation of type-1 DG.

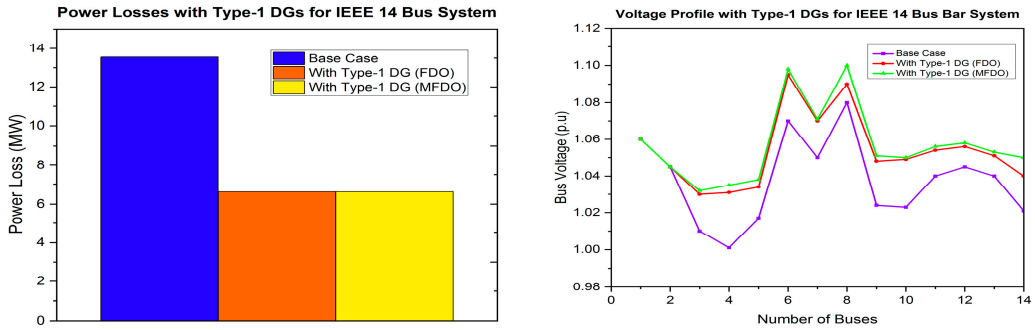

Figure 9. (**a**) Power losses with and without type-1 DG. (**b**) Voltage profile at each bus considering type-1 for the IEEE 14-bus system.

DG can impact the voltage stability of a power system, with acceptable voltage fluctuation limits typically set between 0.95 and 1.1 per unit (p.u.). The results shown in Figure 9b demonstrate that the integration of DG with optimal sizes and locations does not cause voltage fluctuations to exceed these limits. All bus voltages remain within the acceptable range of 0.95 to 1.1 p.u. Using the MFDO method, bus voltages were increased from 1.001 p.u. to at least 1.032 p.u. without any voltage exceeding the permitted limits.

Scenario II: Considering Type-2 DG.

In this case, the DG injected both active and reactive power into the power system. Similarly, when integrating type-2 DG with the optimal placement and sizing which are determined using the proposed MFDO method, power losses are reduced by 62.918%, as shown in Figure 10a. This is a greater reduction compared to the FDO method, which achieved a loss reduction of 62.874%. The MFDO method proves to be more effective in minimizing power losses and is also comparable to other methods used for DG allocation and sizing. Figure 10a illustrates the total power losses calculated after DG integration. It is evident that when a DG unit with a size of 12–0.25 j MVA is installed at bus 10, total power losses are significantly minimized. Specifically, power losses decreased from 13.551 MW to 5.025 MW due to the insertion of type-2 DG. Figure 10a,b compare the power losses and voltage profiles with and without DG, based on both the conventional FDO and the

proposed MFDO methods. Before DG units were integrated, the minimum voltage was approximately 1.001 p.u. in the base case system, indicating that some buses had voltage profiles outside the standard permissible limits. However, after the installation of type-2 DG with optimal sizing and placement, the voltage profile improved from 1.001 p.u. to 1.044 p.u., as shown in Figure 10b.

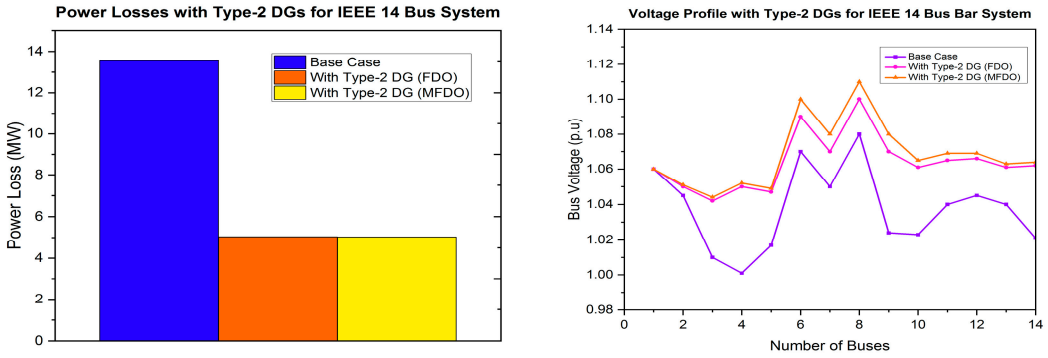

(**a**) (**b**)

Figure 10. (**a**) Power losses with and without type-2 DG. (**b**) Voltage profile at each bus considering type-2 DG for the IEEE 14-bus system.

After integrating type-2 DG optimized using placement and sizing techniques, we analyzed the voltage profile of an IEEE 14-bus test system. The results, illustrated in Figure 10b, show that the integration of DG with optimal sizes and locations maintains voltage levels within acceptable limits, and all bus voltages remain between 0.95 and 1.1 p.u. The MFDO method improved bus voltages from 1.001 p.u. to at least 1.044 p.u., ensuring that no voltage levels exceeded the permitted limits.

Scenario III: Considering Type-3 DG.

In this case, the DG unit only injected active power into the network while absorbing reactive power from external sources. Figure 11a presents the overall power losses after calculation. It is evident that the integration of a DG unit with a capacity of 10 + 1.02 j MVA at bus 8 significantly minimizes overall power losses, reducing them to 6.702 MW. Before the installation of the DG units, the minimum voltage was approximately 0.995 per unit (p.u.) in the base case system. However, following the integration of the appropriately sized type-3 DG at optimal locations, the voltage profile improved from 1.001 to 1.018 per unit (p.u.), as shown in Figure 11b.

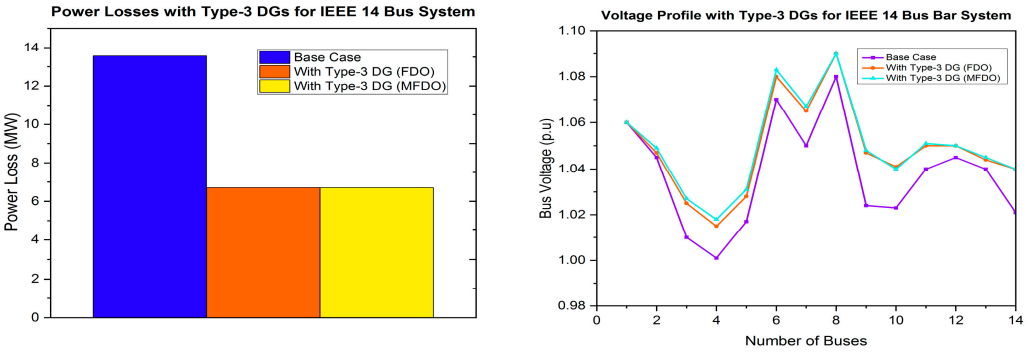

(**a**) (**b**)

Figure 11. (**a**) Power losses with and without type-3 DG. (**b**) Voltage profile at each bus considering type-3 DG for the IEEE 14-bus system.

Scenario IV: Considering Type-4 DG

In a similar manner, Figure 12a displays the calculated power losses. It is evident that integrating a DG unit with a capacity of 1.142 MVAR at bus 13 significantly minimizes power losses, reducing them to 6.107 MW. Before the installation of the DG units, the minimum voltage in the base case system was approximately 0.995 per unit (p.u.). However, after incorporating the appropriately sized type-4 DG at optimal locations, the voltage profile improved from 1.001 to 1.028 per unit (p.u.), as illustrated in Figure 12b.

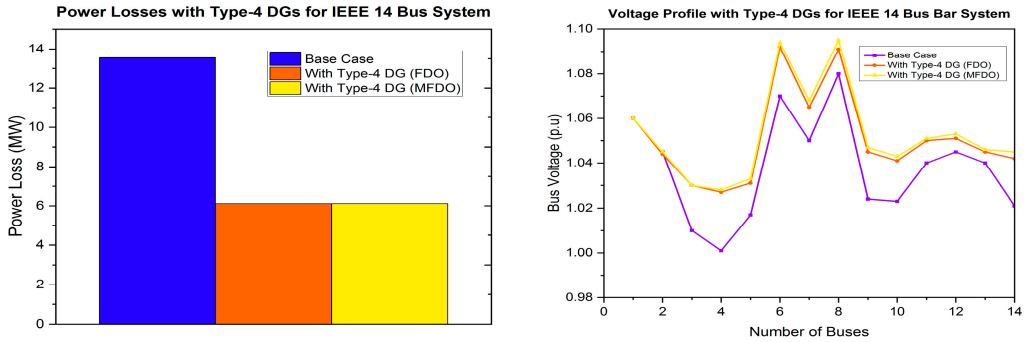

(**a**) (**b**)

Figure 12. (**a**) Power losses with and without type-4 DG. (**b**) Voltage profile at each bus considering type-4 DG for the IEEE 14-bus system.

4.2. Case 2: Simulation Results for Case Study IEEE 30-Bus System

The effectiveness of the proposed method is tested and verified on the 30-bus system. The test system comprises 30 buses, 29 sectionalizing branches, a nominal system voltage of 11 kV, a total active load of approximately 283.4 MW, and a total reactive nature-connected load of about 126.2 MVAR. The system's active power losses in the base case scenario without DG is 17.559 MW, providing a basis for further analysis and comparison with other scenarios. The load flow analysis results without the integration of DG serve as the base case for the 30-bus system and are presented in Tables 3 and 4, as well as Figures 13 and 14.

Table 3. Results of load flow for the 30-bus system without integration of DG.

Bus Node No.	Voltage Magnitude (p.u.)	Phase Angle Degree	Connected Load		Generation Capacity		Injected Reactive Power (MVar)
			MW	MVar	MW	MVar	
1	1.06	0	0	0	260.998	−17.021	0
2	1.043	−5.497	21.7	12.7	40	48.822	0
3	1.022	−8.004	2.4	1.2	0	0	0
4	1.013	−9.661	7.6	1.6	0	0	0
5	1.01	−14.381	94.2	19	0	35.975	0
6	1.012	−11.398	0	0	0	0	0
7	1.003	−13.15	22.8	10.9	0	0	0
8	1.01	−12.115	30	30	0	30.826	0
9	1.051	−14.434	0	0	0	0	0
10	1.044	−16.024	5.8	2	0	0	19
11	1.082	−14.434	0	0	0	16.119	0
12	1.057	−15.302	11.2	7.5	0	0	0
13	1.071	−15.302	0	0	0	10.423	0
14	1.042	−16.191	6.2	1.6	0	0	0
15	1.038	−16.278	8.2	2.5	0	0	0
16	1.045	−15.88	3.5	1.8	0	0	0
17	1.039	−16.188	9	5.8	0	0	0
18	1.028	−16.884	3.2	0.9	0	0	0

Table 3. *Cont.*

Bus Node No.	Voltage Magnitude (p.u.)	Phase Angle Degree	Connected Load		Generation Capacity		Injected Reactive Power (MVar)
			MW	MVar	MW	MVar	
19	1.025	−17.052	9.5	3.4	0	0	0
20	1.029	−16.852	2.2	0.7	0	0	0
21	1.032	−16.468	17.5	11.2	0	0	0
22	1.033	−16.455	0	0	0	0	0
23	1.027	−16.662	3.2	1.6	0	0	0
24	1.022	−16.83	8.7	6.7	0	0	4.3
25	1.019	−16.424	0	0	0	0	0
26	1.001	−16.842	3.5	2.3	0	0	0
27	1.026	−15.912	0	0	0	0	0
28	1.011	−12.057	0	0	0	0	0
29	1.006	−17.136	2.4	0.9	0	0	0
30	0.995	−18.015	10.6	1.9	0	0	0
Total			283.4	126.2	300.998	125.144	23.3

Table 4. Summary of load flow results for a 30-bus system.

Power Loss (MW)	Max Line Loss (MW)	Max Bus Voltage (p.u.)	Min Bus Voltage (p.u.)	Voltage Deviation VD%
17.599	5.464	1.082	0.995	1.9

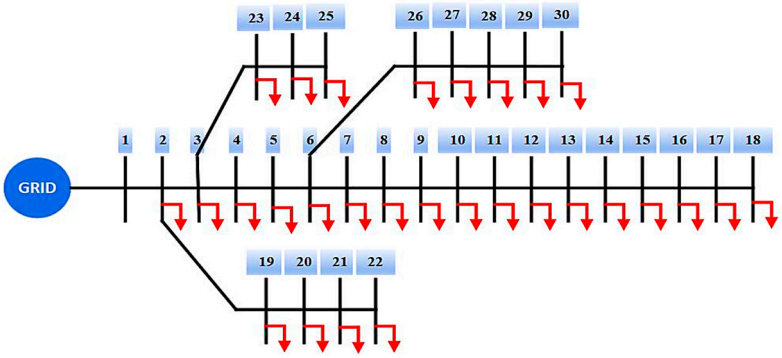

Figure 13. Energy management evaluation on a 30-bus subsystem modeled from IEEE standard 30-bus framework.

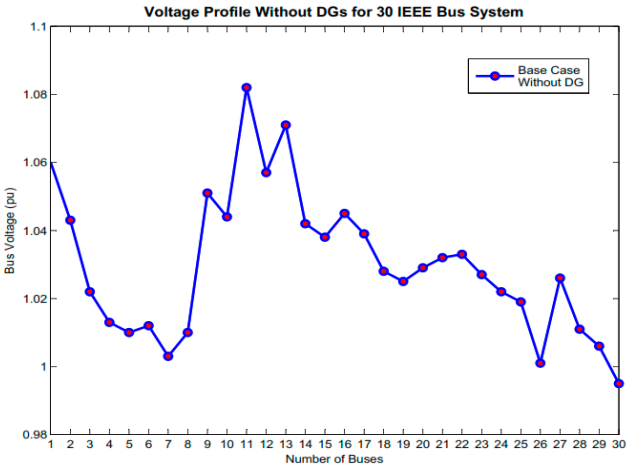

Figure 14. Voltage profile without DG for the IEEE 30-bus system.

Scenario I: Considering Type-1 DG

In this case, the DG unit is only capable of injecting active power into the power system. Figure 15a clearly shows that the conventional FDO method reduced losses by 46.235%, while the proposed MFDO method achieved a reduction of 46.786%. The results obtained with the MFDO technique are superior to those of the FDO technique when considering type-1 DG in the power system. Specifically, when DG units with sizes of 11.6631 MW at bus 10, 11.9985 MW at bus 19, 11.9921 MW at bus 24, and 11.892 MW at bus 30 are integrated, overall power losses are minimized. The power losses decreased from 17.599 MW to 9.3651 MW with the use of type-1 DG.

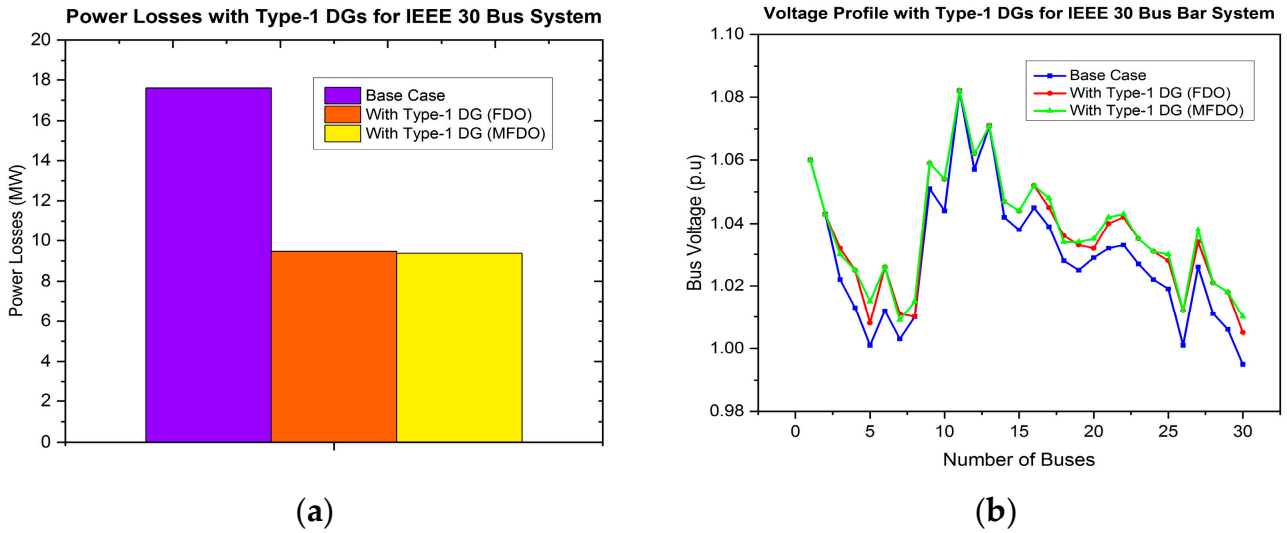

Figure 15. (**a**) Power losses with and without type-1 DG. (**b**) Voltage profile at each bus considering type-1 for the IEEE 30-bus system.

The proposed method increased bus voltages significantly. Before the installation of the DG units, the system's minimum voltage in the base case was approximately 0.995 p.u. This demonstrates that after integrating type-1 DG at optimal locations and with appropriate sizing, the voltage profile improved from 0.995 per unit (p.u.) to 1.008 per unit (p.u.), as shown in Figure 15b.

Scenario II: Considering Type-2 DG

In this case, the DG unit injected both active and reactive power into the power system. When integrating type-2 DG with the optimal placement and sizing which are determined using the proposed MFDO method, power losses are reduced by 64.05%, as shown in Figure 16a. This represents a greater reduction compared to the FDO method, which decreases losses by 63.488%. It is evident that installing DG units with capacities of 12.0365–0.4295 j MVA at bus 18, 11.9825–0.9885 j MVA at bus 20, 11.9289–0.501 j MVA at bus 22, and 11.4951–0.5325 j MVA at bus 30 minimizes total power losses. The power losses decreased from 17.599 MW to 6.3265 MW due to the integration of type-2 DG into the power system.

The results presented in Figure 16b show that after the insertion of a type-2 DG with appropriate size at the optimal locations, the voltage profile improved from 0.995 per unit (p.u.) to 1.011 per unit (p.u.).

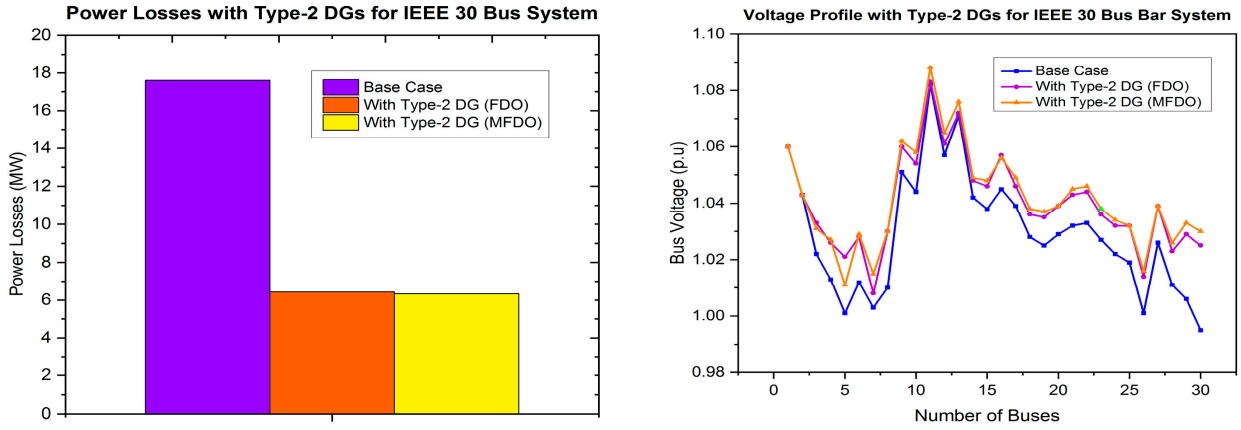

(**a**) (**b**)

Figure 16. (**a**) Power losses with and without type-2 DG. (**b**) Voltage profile at each bus considering type-2 DG for the IEEE 30-bus system.

Scenario III: Considering Type-3 DG

In this case, the DG unit injected only active power into the network while absorbing reactive power from external sources. Additionally, the proposed MFDO technique is employed to determine the optimal sizes and appropriate locations for these DG units.

Figure 17a illustrates that integrating DG units with sizes of 11.862 + 2.5843 j MVA, 11.698 + 3.001 j MVA, 11.865 + 1.2832 j MVA, and 11.963 + 1.4835 j MVA at the appropriate locations of bus 10, bus 17, bus 24, and bus 30, respectively, minimizes overall power losses. Specifically, the incorporation of type-3 DG has reduced power losses to 9.3751 MW. Before the DG units were installed, the minimum voltage in the base case system was approximately 0.995 per unit (p.u.). However, following the installation of type-3 DG at optimal sizes and locations, the voltage profile improved from 0.995 per unit (p.u.) to 1.004 per unit (p.u.), as shown in Figure 17b.

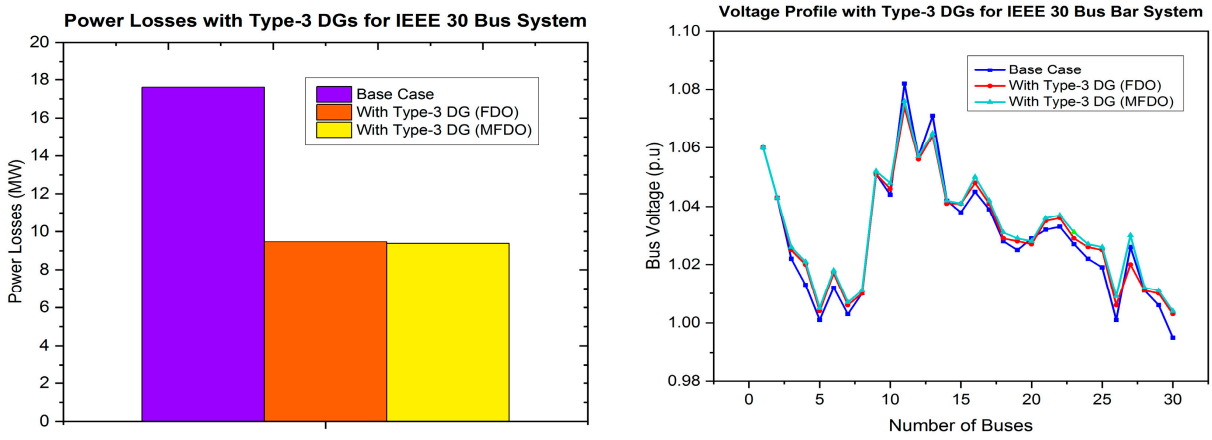

(**a**) (**b**)

Figure 17. (**a**) Power losses with and without type-3 DG for a 30-bus system. (**b**) Voltage profile at each bus considering type-3 DG for the IEEE 30-bus system.

Scenario IV: Considering Type-4 DG

In a similar manner, it is evident that when integrating DG units with sizes of 1.6223 MVAR at bus 10, 1.7249 MVAR at bus 15, 1.8198 MVAR at bus 22, and 1.9024 MVAR at bus 30, the power losses become minimized, as illustrated in Figure 18a. Specifically, the incorporation of type-4 DG has reduced power losses to 8.165 MW.

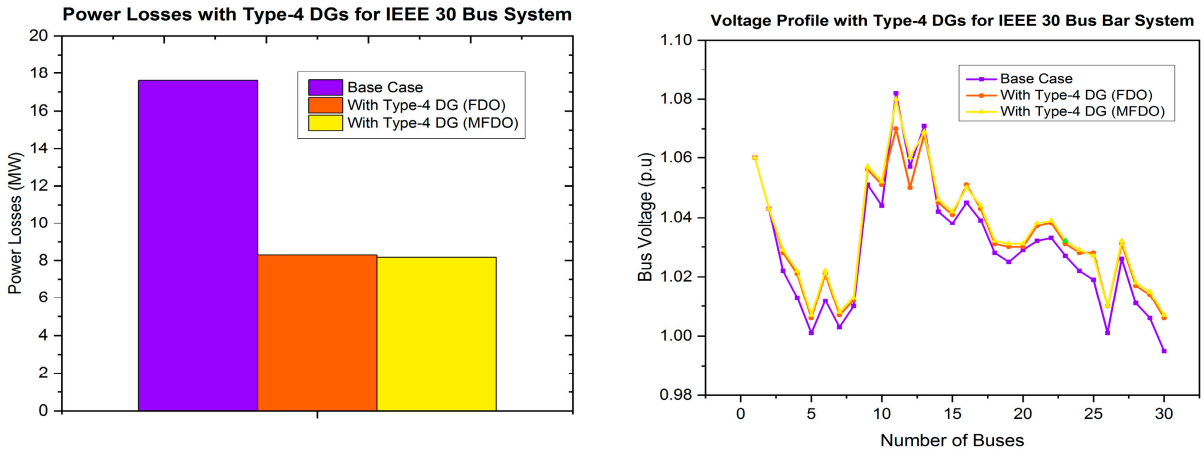

(**a**) (**b**)

Figure 18. (**a**) Power losses with and without type-4 DG. (**b**) Voltage profile at each bus considering type-4 DG for the IEEE 30-bus system.

Before the installation of these DG units, the minimum voltage in the base case system was approximately 0.995 per unit (p.u.). However, after installing type-4 DG units at optimal sizes and locations, the voltage profile improved from 0.995 to 1.007 per unit (p.u.), as shown in Figure 18b.

5. Discussion

This section provides a summary of the results, compares them with conventional methods from other authors, and discusses their interpretation in the context of previous studies and the working hypotheses. The findings and their implications are also discussed in this section.

5.1. Comparison of Proposed Method Results with Other Available Methods for the IEEE 14 Bus System

In this section, the IEEE 14-bus benchmark test system has been considered by integrating different types of DGs to implement and analyze the proposed method, assessing its validity and effectiveness compared to other available methods.

Scenario I: Considering Type-1 DG

In this case, the DG is capable of injecting only active power into the system. Before the installation of DG units, the system's minimum voltage under the base case was approximately 1.001p.u., indicating that some buses exceeded the defined voltage limits. It is evident that when a DG unit of 11.89 MW is placed at bus 2, overall power losses are minimized. The active power losses decreased from 13.599 MW to 6.641 MW with the integration of type-1 DG, as shown in Figure 9a. Furthermore, after incorporating type-1 DG with an appropriate size at optimal locations, which is optimized using the MFDO technique, the voltage profile improved from 1.001 per unit (p.u.) to 1.032 per unit (p.u.), as seen in Figure 9b and Table 5.

The integration of DG not only enhanced the voltage profiles of the targeted buses but also significantly improved the profiles of other weak buses. A comparison of voltage profiles and power losses using different methods is presented in Table 5 and Figure 19.

Table 5. Comparison of voltage drops and power losses using type-1 DG for the IEEE 14-bus system.

Performance Parameters	Approach					
	Base Case	GA [77]	PSO [78]	IPSO [79]	Hybrid GA-IPSO [80]	Proposed MFDO
Optimal Sizes (MW)/Location	-	11.86/9	12.01/10	12.32/13	14.12/14	11.89/2
Active Power Loss (MW)	13.551	10.311	9.4423	9.3827	8.1631	6.641
Power Loss Reduction	-	3.24	4.1087	4.1683	5.3879	6.911
Power Loss Reduction (%)	-	23.910	30.320	30.760	39.760	50.99
Minimum Voltage (P.U.)	1.001	0.925	0.986	1.011	1.024	1.032
Maximum Voltage (P.U.)	1.080	1.085	1.087	1.089	1.091	1.099

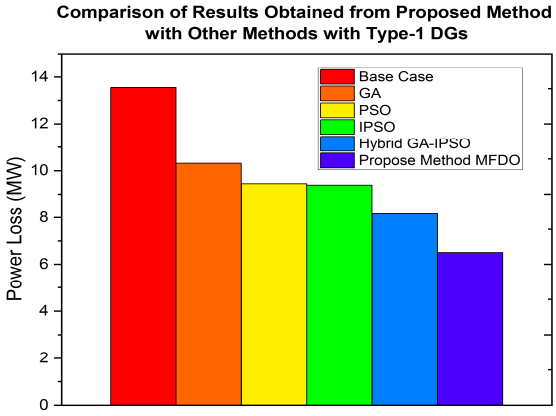

Figure 19. Power losses comparison of type-1 DG with conventional and proposed methods for the IEEE 14-bus system.

Scenario II: Considering Type-2 DG

In this scenario, the improvements in the voltage profile and reductions in power losses are better as compared to the previous case with type-1 DG. This is due to the ability of this type of DG to inject reactive power, which helps enhance the node voltage profile. Additionally, it significantly reduces the line current supplied by the grid source, leading to minimum line losses as a result of reduced current. A comparison of the voltage profile and power losses using different methods is provided in Table 6 and shown in Figure 20.

Table 6. Comparison of voltage drops and power losses with considering type-2 DG for the IEEE 14-bus system.

Performance Parameters	Approach					
	Base Case	GA [77]	PSO [78]	IPSO [79]	Hybrid GA-IPSO [80]	Proposed MFDO
Optimal Sizes (MVA)/Location	-	11.85–0.78 j/9	12.52–0.56 j/10	12.49–0.51 j/13	14.65–0.86 j/14	12–0.25 j/10
Active Power Loss (MW)	13.551	8.8759	8.5507	8.3035	7.8555	5.025
Power Loss Reduction	-	4.6751	5.0003	5.2475	5.6955	8.526
Power Loss Reduction (%)	-	34.500	36.900	38.724	42.030	62.918
Minimum Voltage (P.U.)	1.001	0.936	0.989	1.001	1.002	1.044
Maximum Voltage (P.U.)	1.080	1.091	1.092	1.096	1.099	1.10

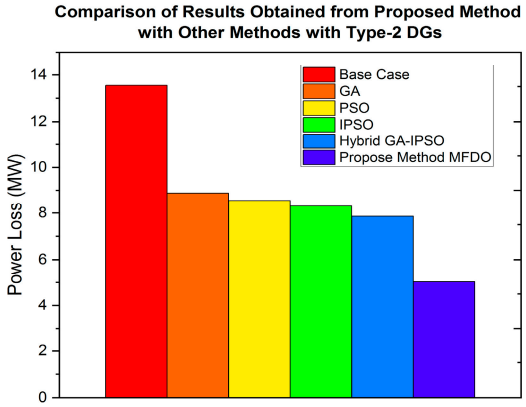

Figure 20. Power losses comparison of type-2 DG with conventional and proposed methods for the IEEE 14-bus system.

Scenario III: Considering Type-3 DG

In this case, when comparing this scenario to the second one, it is observed that the percentages of power loss reduction and voltage profile improvement are not much better than those achieved with type-2 DG. This is due to the reactive power demand absorbed by this type of DG, which helps improve the node's voltage profile. However, when compared to the base case, the results show that the voltage profiles of most buses have improved and power losses have decreased. A comparison of voltage profiles and power losses using different methods is presented in Table 7 and Figure 21.

Table 7. Comparison of voltage drops and power losses with considering type-3 DG for the IEEE 14-bus system.

Performance Parameters	Approach					
	Base Case	**GA [77]**	**PSO [78]**	**IPSO [79]**	**Hybrid GA-IPSO [80]**	**Proposed MFDO**
Optimal Sizes (MVA)/Location	-	11.45 + 1.16 j/9	12.03 + 1.27 j/10	12.19 + 1.34 j/13	14.15 + 1.57 j/14	10 + 1.02 j/8
Active Power Loss (MW)	13.551	10.479	9.3217	9.2133	8.7783	6.702
Power Loss Reduction	-	3.072	4.2293	4.3377	4.7727	6.849
Power Loss Reduction (%)	-	22.670	31.210	32.010	35.220	50.542
Minimum Voltage (P.U.)	1.001	0.945	0.989	1.002	1.003	1.018
Maximum Voltage (P.U.)	1.080	1.081	1.082	1.084	1.088	1.091

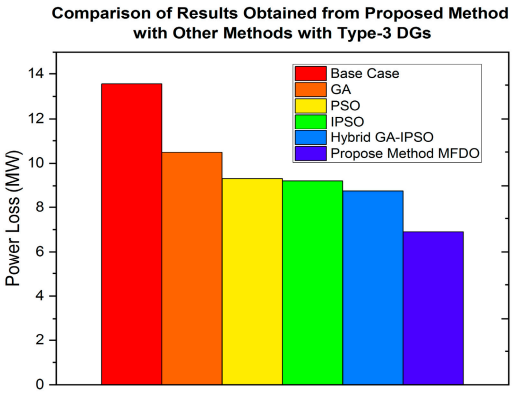

Figure 21. Power losses comparison of type-3 DG with conventional and proposed methods for the IEEE 14-bus system.

Scenario IV: Considering Type-4 DG

In this case, when comparing this case to the third scenario, it is determined that the percentages of power loss reduction and voltage profile improvement are better than those achieved with type-3 DG in the previous case. A comparison of voltage profiles and power losses using different methods is provided in Table 8 and Figure 22.

Table 8. Comparison of voltage drops and power losses using type-4 DG for the IEEE 14-bus system.

Performance Parameters	Approach					
	Base Case	GA [77]	PSO [78]	IPSO [79]	Hybrid GA-IPSO [80]	Proposed MFDO
Optimal Sizes (MVAR)/Location	-	1.843/9	1.683/10	1.568/13	1.502/14	1.142/13
Active Power Loss (MW)	13.551	10.575	9.7676	9.5833	8.2404	6.107
Power Loss Reduction	-	2.976	3.7834	3.9677	5.3106	7.44
Power Loss Reduction (%)	-	21.961	27.920	29.280	39.190	54.93
Minimum Voltage (P.U.)	1.001	0.915	0.936	0.952	0.957	1.028
Maximum Voltage (P.U.)	1.080	1.081	1.083	1.087	1.092	1.095

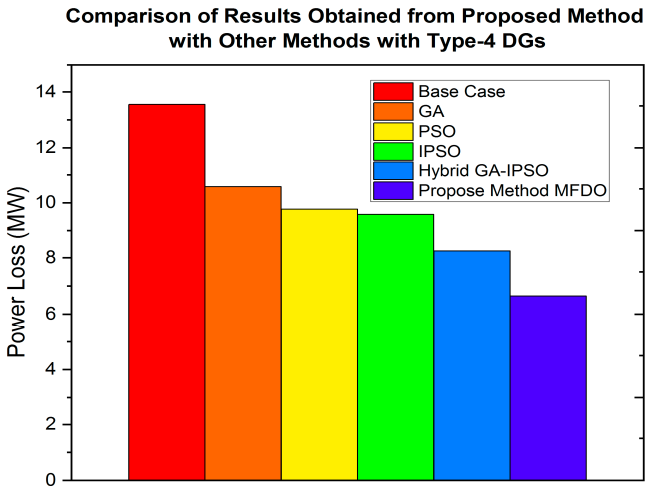

Figure 22. Power loss comparison of type-4 DG with conventional and proposed methods for the IEEE 14-bus system.

5.2. Results Summary for the IEEE 14-Bus System

This section examines the impact of integrating different types of DG technology on the voltage profile and power system losses and determines the optimal placement and sizes using the proposed MFDO technique. The effects on power losses and voltage variations in different types of DGs such as type-1, type-2, type-3, and type-4 are illustrated in Figures 9–12, respectively. When comparing type-2 DG with other types, it is evident that the integration of type-2 DG results in lower power system losses and greater voltage profile improvements compared to the other types (type-1, type-3, and type-4), as shown in the figures. Power losses are shown in Figures 23 and 24, while the voltage profile in Figure 25 provides a better visualization of how type-2 DG achieves lower power losses and a higher voltage profile than the other types.

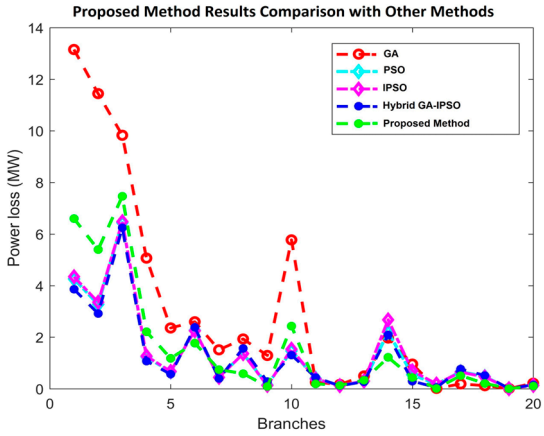

Figure 23. Power losses comparison on each branch with and without DG of optimization results using different methods for the IEEE 14-bus system.

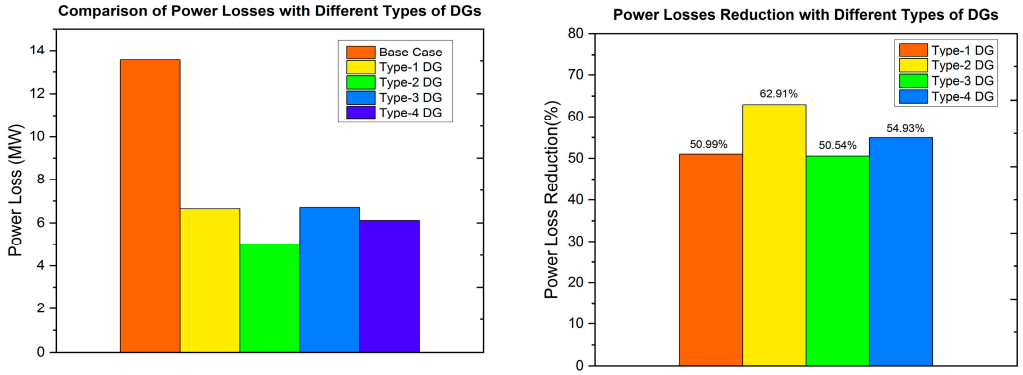

(**a**) (**b**)

Figure 24. (**a**) Total power losses comparison of optimization results with different types of DGs. (**b**) Power losses reduction (%) comparison of optimization results with different types of DGs for the IEEE 14-bus system.

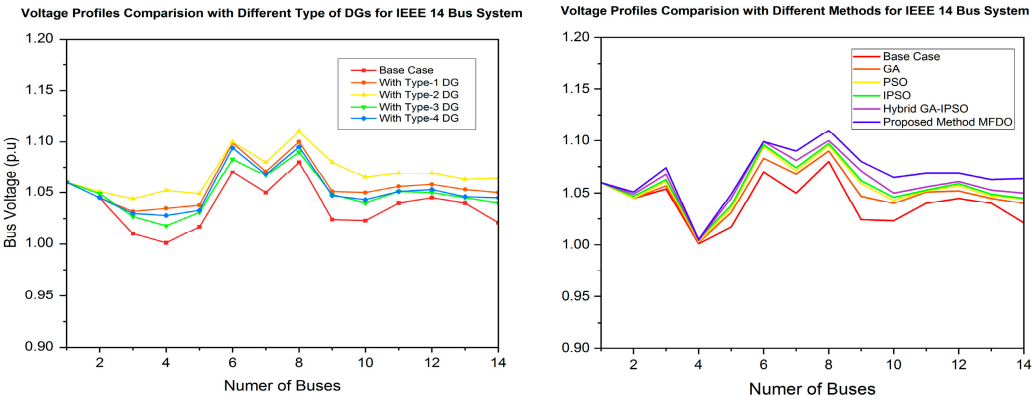

(**a**) (**b**)

Figure 25. (**a**) Voltage profiles comparison at each bus with and without DG using different types of DGs. (**b**) Voltage profiles comparison with different conventional and proposed methods for the IEEE 14-bus system.

The summary of results for all scenarios is presented in Figure 24a,b. It can be observed that the integration of type-2 DG into the power system yields better results than the other types (such as type-1, type-3, and type-4 DG). To verify the validity of the new results

obtained using the proposed MFDO technique, it is essential to compare them with previous results from conventional methods. The proposed MFDO method achieved significantly better outcomes in terms of power loss reduction, as shown in Figure 24b. Specifically, power losses decreased by 62.874% using the FDO method and by 62.918% with the MFDO method. Moreover, when applying the proposed optimization approach, the required DG unit capacity is minimized.

The voltage profile comparison for different scenarios in the IEEE 14-bus test system is presented in Table 9. Figure 25 illustrates the bus voltage comparisons when using the conventional methods and the proposed MFDO technique to determine the optimal sizes and placements while considering type-2 DG. The table shows that, when the proposed MFDO technique is taken into consideration, all bus voltages have improved and are within acceptable limits. MATLAB software 2018 is used to implement the proposed system, and the simulation plots for the voltage profile comparison are shown in Figure 25.

Table 9. Results summary for all types DG scenarios for the IEEE 14-bus system.

Performance Parameters	Scenarios				
	Base Case	Type-1 DG	Type-2 DG	Type-3 DG	Type-4 DG
Active Power Loss (MW)	13.551	6.641	5.025	6.702	6.107
Minimum Voltage (P.U.)	1.001	1.032	1.044	1.018	1.028
Maximum Voltage (P.U.)	1.080	1.099	1.1	1.091	1.095
Voltage Deviation (%)	4.16	3.4	3.2	3.5	3.6
Power Loss Reduction (%)	-	50.99%	62.91%	50.54%	54.93%

It is evident that the proposed approach is more effective for integrated DG power systems in improving the voltage profile. This occurs because the current injected by the installed DG reduces the line current drawn from the grid source, which in turn decreases the voltage drop and helps improve both the voltage profile and stability, as shown in Figure 26 below.

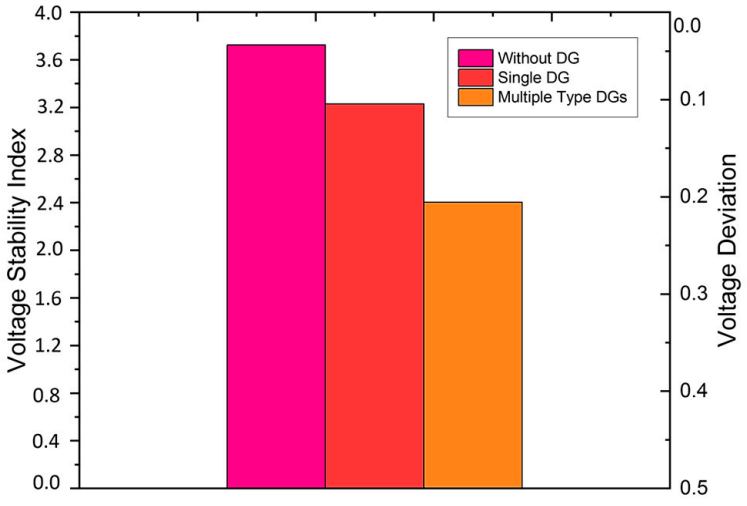

Figure 26. Voltage stability index comparison with and without DG using the proposed method for the IEEE 14-bus system.

Table 9 summarizes the power losses and bus voltages for the proposed methods. Comparing the results of the MFDO method to conventional methods, while considering different types of DG, is crucial for validating the proposed methodology. Table 9 shows that the MFDO method achieves greater power loss reductions and voltage profile improvements compared to conventional methods, specifically when considering type-2 DG in the IEEE 14-bus system. This indicates that when the proposed MFDO optimization approach

is applied, all bus voltages remain within the acceptable threshold values, power losses are minimized, and the required DG unit capacities are smaller. As a result, this approach not only reduces costs but also increases system efficiency.

5.3. Comparison of Proposed Method Results with Other Available Methods for the IEEE 30 Bus System

In this section, the IEEE 30-bus benchmark test system has been considered by integrating different types of DGs for the implementation and analysis to check the proposed method's validity and effectiveness compared with other available methods.

Scenario I: Considering Type-1 DG

In this scenario, the values of voltage profile improvements and power loss reductions are better as compared to the previous base case. The comparison of voltage profile and power losses with different methods for the IEEE 30-bus system is shown in Table 10 and Figure 27.

Table 10. Comparison of voltage drops and power losses using type-1 DG for the IEEE 30-bus system.

Performance Parameters	Approach					
	Base Case	GA [77]	PSO [78]	IPSO [79]	Hybrid GA-IPSO [80]	Proposed MFDO
Optimal Sizes (MW)/Location	-	11.472/10 11.904/10 11.052/19 11.772/24	11.694/10 11.394/15 11.378/20 10.577/30	11.625/10 11.956/10 11.995/22 11.986/30	11.7099/19 11.9937/21 11.9960/24 11.7061/30	11.6631/10 11.9985/19 11.9921/24 11.8920/30
Active Power Loss (MW)	17.599	13.3919	12.2622	12.1851	10.6020	9.3651
Power Loss Reduction	-	4.4879	5.6176	5.6947	6.2778	8.2339
Power Loss Reduction (%)	-	25.1002	31.4187	31.8499	40.7040	46.786
Minimum Voltage (P.U.)	0.995	0.98	0.988	0.99	1.005	1.008
Maximum Voltage (P.U.)	1.082	1.081	1.082	1.084	1.085	1.086

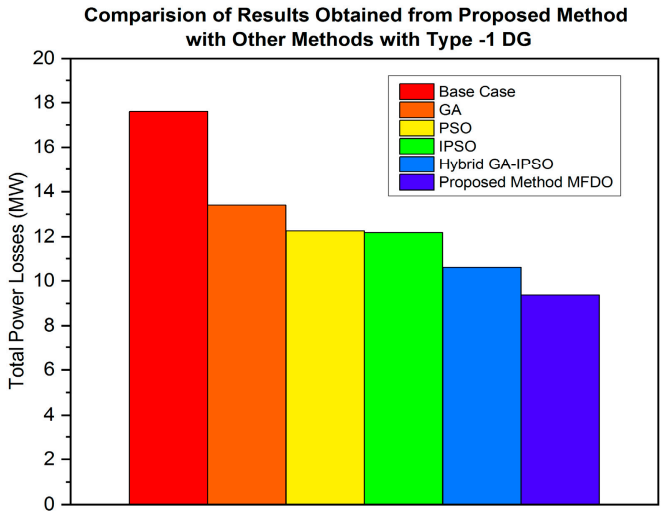

Figure 27. Power losses comparison of type-1 DG with conventional and proposed methods for the IEEE 30-bus system.

Scenario II: Considering Type-2 DG

In this scenario, the improvements in the voltage profile and reductions in power losses are better as compared to the previous case with type-1 DG. This is due to the ability

of this type of DG to inject reactive power, which helps enhance the node voltage profile. Additionally, it significantly reduces the line current supplied by the grid source, leading to minimum line losses as a result of reduced current. A comparison of the voltage profile and power losses using different methods is provided in Table 11 and shown in Figure 28.

Table 11. Comparison of voltage drops and power losses with considering type-2 DG for the IEEE 30-bus system.

Performance Parameters	Approach					
	Base Case	GA [77]	PSO [78]	IPSO [79]	Hybrid GA-IPSO [80]	Proposed MFDO
Optimal Sizes (MVA)/Location	-	9.038–0.088 j/10 11.112–0.715 j/18 11.748–0.589 j/22 10.008–0.487 j/30	11.88–0.79 j/10 10.88–0.32 j/18 11.56–0.89 j/20 11.53–0.38 j/30	12.02–0.52 j/10 10.86–0.30 j/19 11.91–0.83 j/22 11.95–0.52 j/30	12.01–0.48 j/19 11.94–0.50 j/21 11.91–0.06 j/24 11.36–0.58 j/30	12.0365–0.4295 j/18 11.9825–0.4985 j/20 11.9289–0.0501 j/22 11.4951–0.5325 j/30
Active Power Loss (MW)	17.599	11.5265	11.1056	11.2099	10.2021	6.3265
Power Loss Reduction	-	6.3533	6.772	6.6699	7.6777	11.2725
Power Loss Reduction (%)	-	35.6967	37.8874	37.3041	42.9406	64.05
Minimum Voltage (P.U.)	0.995	1.006	0.988	1.002	1.007	1.011
Maximum Voltage (P.U.)	1.082	1.086	1.087	1.088	1.088	1.09

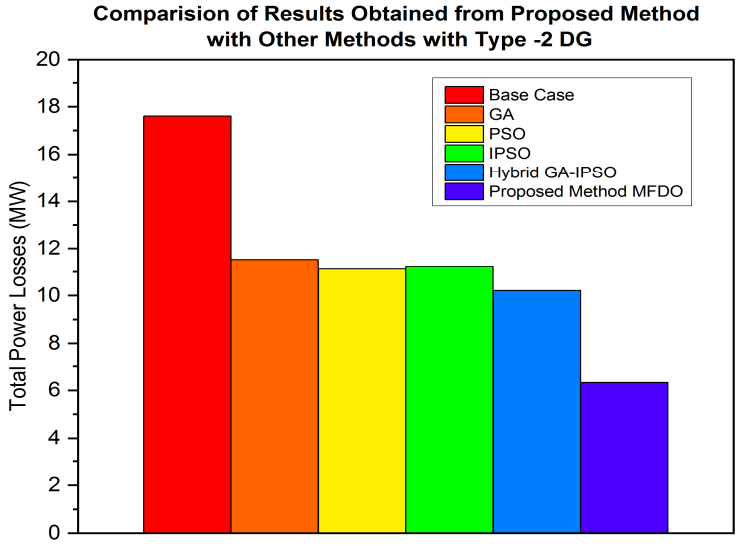

Figure 28. Power losses comparison of type-2 DG with conventional and proposed methods for the IEEE 30-bus system.

Scenario III: Considering Type-3 DG

In this case, when comparing this case to the second scenario, it is found that the percentages of power loss reduction and voltage profile improvement are not significantly better than those achieved with type-2 DG. However, compared to the base case, the results show that the voltage profiles of most buses have improved, and power losses have been reduced. A comparison of voltage profiles and power losses using different methods is provided in Table 12 and Figure 29.

Table 12. Comparison of voltage drops and power losses with considering type-3 DG for the IEEE 30-bus system.

Performance Parameters	Approach					
	Base Case	GA [77]	PSO [78]	IPSO [79]	Hybrid GA-IPSO [80]	Proposed MFDO
Optimal Sizes (MVA)/Location	-	11.35 + 1.22 j/10 11.47 + 1.17 j/23 11.92 + 2.04 j/24 11.816 + 1.468 j/30	11.474 + 2.159 j/10 11.981 + 0.919 j/17 11.67 + 2.309 j/20 11.349 + 3 j/30	11.83 + 0.001 j/10 11.433 + 3 j/21 11.739 + 3 j/24 11.955 + 0.001 j/30	11.7872 + 2.9609 j/19 11.7548 + 3.002 j/23 12 + 1.3702 j/24 11.8303 + 1.5817 j/30	11.862 + 2.5843 j/10 11.698 + 3.001 j/17 11.865 + 1.2835 j/24 11.963 + 1.4835 j/30
Active Power Loss (MW)	17.599	12.2260	12.1060	11.9500	11.4001	9.3751
Power Loss Reduction	-	5.6538	5.7738	5.9298	6.4797	8.2239
Power Loss Reduction (%)	-	31.5890	32.2923	33.1648	36.2403	46.729
Minimum Voltage (P.U.)	0.995	0.97	0.98	0.988	1.001	1.004
Maximum Voltage (P.U.)	1.082	1.072	1.074	1.075	1.075	1.076

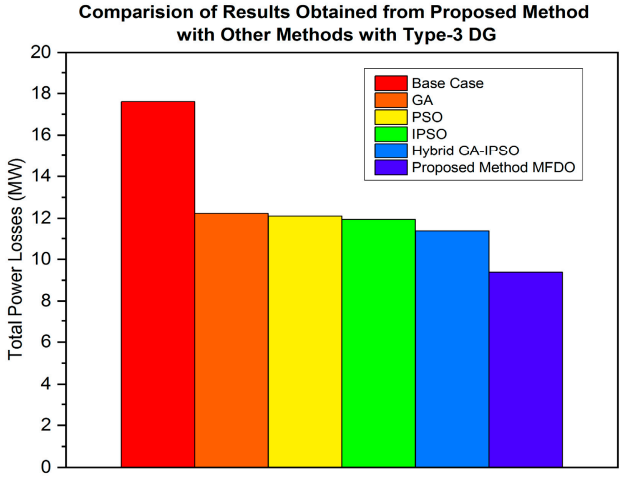

Figure 29. Power losses comparison of type-3 DG with conventional and proposed methods for the IEEE 30-bus system.

Scenario IV: Considering Type-4 DG

In this case, when comparing this case to the third scenario, it is determined that the percentages of power loss reductions and voltage profile improvements are better than previous case type-3 DG. The comparison of voltage profile and power losses with different methods is shown in Table 13 and Figure 30.

Table 13. Comparison of voltage drops and power losses using type-4 DG for the IEEE 30-bus system.

Performance Parameters	Approach					
	Base Case	GA [77]	PSO [78]	IPSO [79]	Hybrid GA-IPSO [80]	Proposed MFDO
Optimal Sizes (MVAR)/Location	-	3.0985/10 2.8862/18 3.6878/22 2.5876/30	3.8354/10 3.4763/18 1.9274/20 2.4873/30	2.9349/10 3.9738/19 1.9347/22 2.9454/30	1.9394/19 2.9245/21 1.9184/24 2.9247/30	1.6223/10 1.7249/15 1.8198/22 1.9024/30
Active Power Loss (MW)	17.599	13.7351	12.4463	12.6852	10.7020	8.165
Power Loss Reduction	-	4.4879	5.6176	5.6947	6.2778	9.434
Power Loss Reduction (%)	-	25.1002	31.4187	31.8499	40.7040	53.605
Minimum Voltage (P.U.)	0.995	0.998	1.002	1.001	1.002	1.007
Maximum Voltage (P.U.)	1.082	1.076	1.078	1.079	1.081	1.082

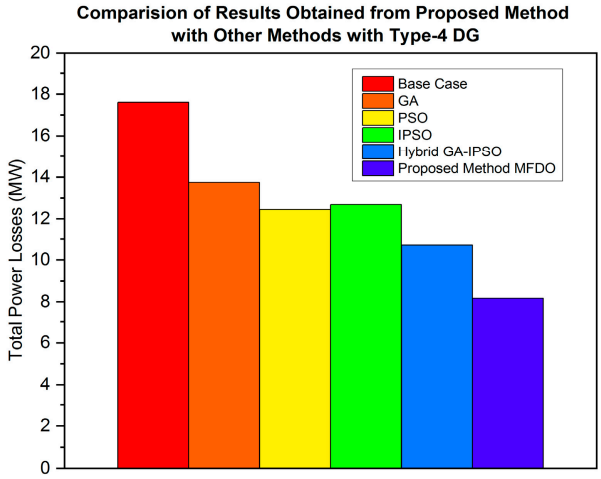

Figure 30. Power losses comparison of type-4 DG with conventional and proposed methods for the IEEE 30-bus system.

5.4. Results Summary for the IEEE 30-Bus System

This section examines the impact of integrating different types of DG technology, along with their optimal sizes and placements, on the voltage profile and power system losses. The effects on power losses and voltage variations for various types of DGs such as type-1, type-2, type-3, and type-4 are illustrated in Figures 15–18, respectively. When comparing type-2 DG with other types, it is found that integrating type-2 DG results in lower power system losses and a higher voltage profile improvement ratio compared to the other types (type-1, type-3, and type-4), as shown in the figures. For better visualization, the power losses are shown in Figures 31 and 32, while the voltage profile is presented in Figure 33, demonstrating how type-2 DG achieves lower losses and a higher voltage profile than the other types.

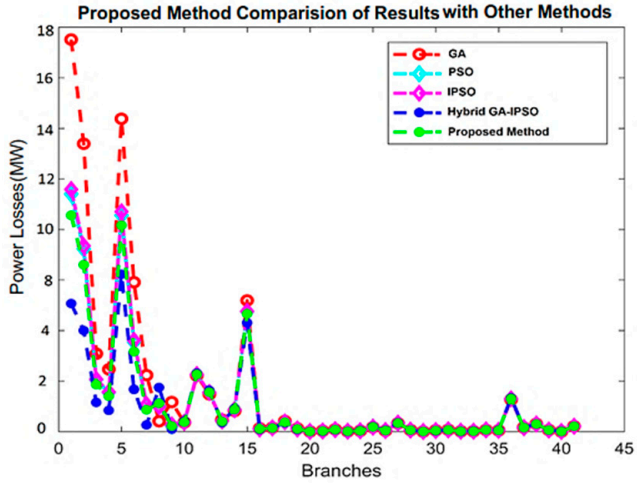

Figure 31. Power losses comparison on each branch with and without DG of optimization results using different methods for the IEEE 30-bus system.

The results summary for all scenarios is presented in Figure 32a,b. It can be observed that the integration of type-2 DG into the power system produces better outcomes than other types (such as type-1, type-3, and type-4 DG). To verify the validity of the new results obtained using the proposed MFDO technique, it is important to compare them with previous results from conventional methods. The proposed MFDO method achieved much better reductions in power losses, as shown in Figure 32b. Specifically, power losses decreased by 63.488% using the FDO method and by 64.051% with the proposed MFDO

method. Additionally, the proposed optimization approach minimizes the required capacity of DG units.

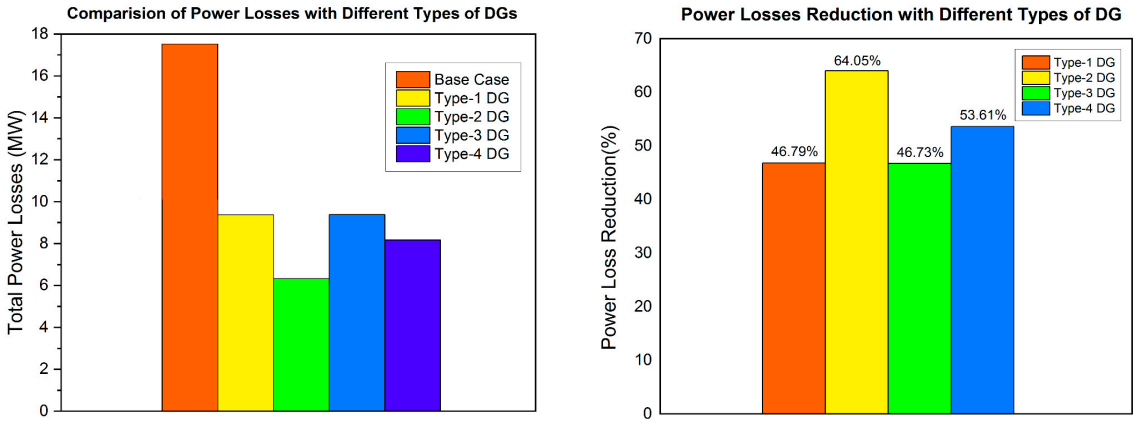

Figure 32. (**a**) Total power losses comparison of optimization results with different types of DGs. (**b**) Power loss reduction (%) comparison of optimization results with different types of DGs for the IEEE 30-bus system.

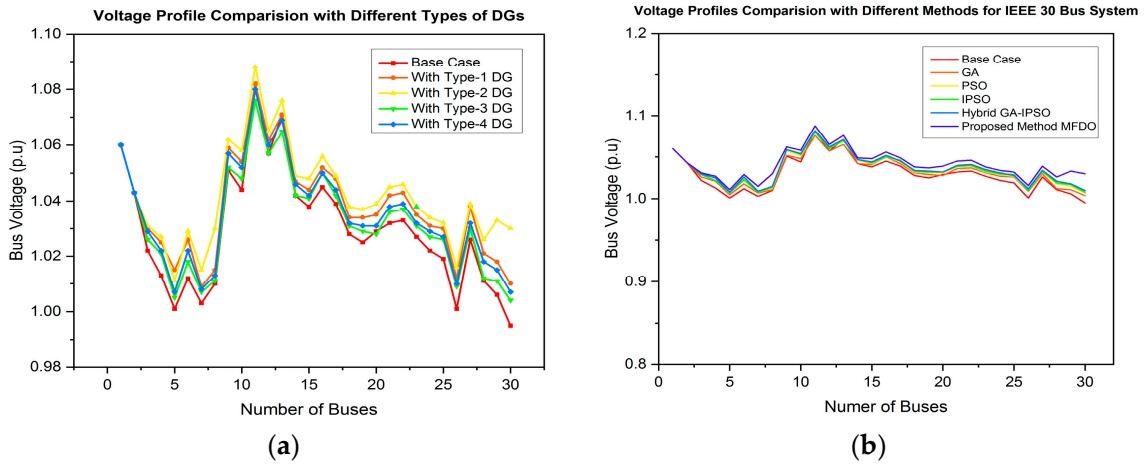

Figure 33. (**a**) Voltage profile comparison at each bus with and without DG using different types of DG. (**b**) Voltage profiles comparison with different conventional and proposed methods for the IEEE 30-bus system.

The voltage profile comparison for different scenarios in the IEEE 30-bus test system is presented in Table 14. Figure 33 illustrates the bus voltage comparisons when using conventional methods and the proposed MFDO technique to determine the optimal sizes and placements while considering type-2 DG. The table shows that, when the proposed MFDO technique is taken into consideration, all bus voltages have improved and are within acceptable limits. MATLAB software is used to implement the proposed system, and the simulation plots for the voltage profile comparison are shown in Figure 33. It is evident that the proposed approach is more effective for integrated DG power systems in improving the voltage profile.

Table 14. Results summary for all types of DG scenarios for the IEEE 30-bus system.

Performance Parameters	Scenarios				
	Base Case	Type-1 DG	Type-2 DG	Type-3 DG	Type-4 DG
Active Power Loss (MW)	17.559	9.3651	6.3265	9.3751	8.165
Minimum Voltage (P.U.)	0.995	1.008	1.011	1.004	1.007
Maximum Voltage (P.U.)	1.082	1.086	1.090	1.076	1.082
Voltage Deviation (%)	1.9	1.4	1.2	1.5	1.6
Power Loss Reduction (%)	-	46.78%	64.05%	46.72%	53.60%

This is because the current injected by the installed DG reduces the line current drawn from the grid source, which in turn decreases the voltage drop and enhances both the voltage profile and system stability, as shown in Figure 34 below.

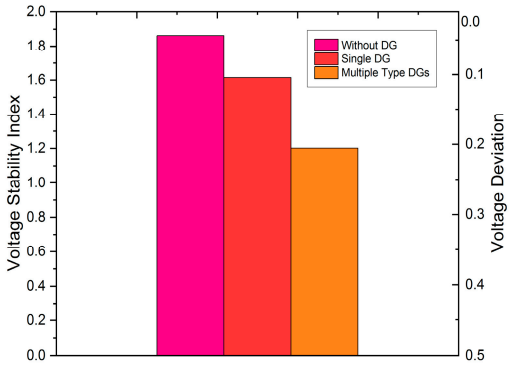

Figure 34. Voltage stability index comparison with and without DG using the proposed method for the IEEE 30-bus system.

Table 14 summarizes the power losses and bus voltages for the proposed methods. Comparing the results of the MFDO method to conventional methods, while considering different types of DG, is crucial for validating the proposed methodology.

Table 14 shows that the MFDO method achieves greater power loss reductions and voltage profile improvements compared to conventional methods, specifically when considering type-2 DG in the IEEE 30-bus system. This indicates that when the proposed MFDO optimization approach is applied, all bus voltages remain within the acceptable threshold values, power losses are minimized, and the required DG unit capacities are smaller. As a result, this approach not only reduces costs but also increases system efficiency.

5.5. Convergence Evaluation

The simulation results demonstrate that the proposed MFDO can provide the desired optimal solutions with minimal computing time as compared to conventional techniques such as GA, PSO, IPSO, Hybrid GAIPSO, and original FDO, etc. Tables 15 and 16 show the parameters for both the conventional and proposed MFDO algorithms, which are set as follows: maximum iterations = 100, maximum generation (runs) = 60, and population size (number of scout bees) = 30.

Table 15. Parameters for conventional methods.

Parameters	Conventional Other Methods Parameters		
	PSO	IPSO	Hybrid GAIPSO
C1	2	0.5	1.2
C2	2	0.5	1.2
W_{min}	0.5	0.5	0.4
W_{max}	0.8	0.8	0.9

Table 15. *Cont.*

Parameters	Conventional Other Methods Parameters		
	PSO	**IPSO**	**Hybrid GAIPSO**
Population	100	50	50
Maximum generation (run)	1000	500	200
Number of Swarm	300	200	100
Maximum No. of iterations	400	300	150
No. of Partial Solutions	50	50	30

Table 16. Parameters for proposed methods.

Parameters	Proposed FDO and MFDO Method Parameters	
	FDO	**MFDO**
Random walk (r)	$[-1, 1]$	$[0, 1]$
Lower Bound (L_b)	-2	-2
Upper Bound (U_b)	2	2
Population size (number of scout bees)	30	10
Maximum generation (run)	100	60
Number of dimensions	9	5
Maximum no. of iterations (t_{max})	100	100
Weight factor (wf)	[1, 0]	[0, 0.2]

The convergence characteristics and execution time of the proposed method are significantly better than those of conventional methods. The comparison of conventional methods and the proposed approach with multiple DG units is shown in Table 17 and Figure 35. Figure 35 illustrates that the convergence rate of the proposed MFDO is higher than that of the conventional FDO and other methods. This improvement in convergence is achieved by incorporating the sinc method into the proposed approach, which updates the fw, which affects the *pace* value and shrinks the range of wf.

Table 17. Comparison of execution time with conventional and proposed methods.

Various Approaches	Comparison of Execution Time with Conventional and Proposed Methods
	Total Average Time (s)
LF	108.036
GA	28.795
PSO	21.940
IPSO	19.864
Hybrid GA + IPSO	22.119
Proposed Method (MFDO)	10.021

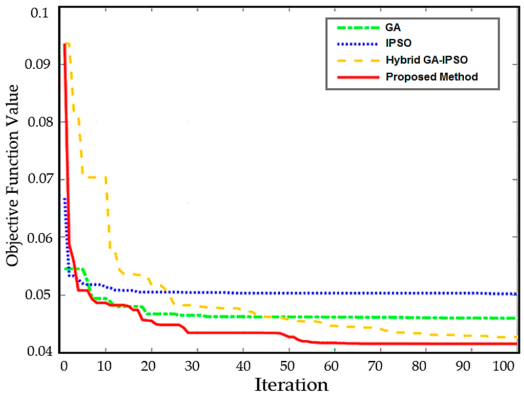

Figure 35. Convergence characteristics comparison of conventional and proposed method with multi DG units.

6. Conclusions and Recommendations

The integration of modern renewable energy sources based on distributed generation (DG) into electrical distribution networks plays an important role in addressing power system profile issues related to increasing load demands, poor supply quality, and unreliability. However, the arbitrary installation of DG in power systems can lead to several adverse effects, including voltage fluctuations, increased power losses, frequency variations, and potential instability of the power system. Proper integration of DG with appropriate sizing and placement offers a credible solution to various challenges in distributed networks. To maximize the techno-economic benefits of DG, it is essential to allocate the DG units at optimal locations and sizes. This research proposes a computational intelligence approach based on the Modified Fitness-Dependent Optimizer (MFDO) technique to identify suitable sizes and optimal placements for newly introduced DG within a network. The approach utilizes an optimized multi-objective framework that includes parameters such as voltage profile improvement, power loss minimization, and stability enhancement. The proposed method is robust, efficient, and converges faster than conventional techniques, making it an inspiring solution for efficient optimization. The performance and feasibility of the proposed framework are analyzed and tested on standard 14-bus and 30-bus benchmark test systems using MATLAB. The results indicate that, following the integration of DG with appropriate sizes at optimal locations, the power losses in the 14-bus system are reduced by up to 5.025 MW (reduction is in percentage approximately by up to 62.91%), and the voltage profile improves from 1.001 per unit (p.u.) to 1.044 per unit (p.u.). Similarly, in the 30-bus system, the power losses decrease by up to 11.2725 MW (reduction is in percentage approximately by up to 64.051%), with the voltage profile improving from 0.955 per unit (p.u.) to 1.088 per unit (p.u.). These findings demonstrate that the proposed method significantly enhances the performance of the power system compared to conventional methods, resulting in substantial reductions in power losses and notable improvements in the voltage profiles of network buses through the integration of multiple DG units with appropriate sizes at optimal locations.

Future Recommendations

The various aspects of the work presented in this paper can be expanded for future research, with several potential directions outlined below:

- Future studies could explore the application of this method with new objective functions and nature-inspired techniques. The efficiency of the proposed method may also be enhanced through potential modifications and new application areas.
- A new variant of the Fitness-Dependent Optimizer (FDO) could be developed or utilized to address multi-objective problems. Researchers may also be interested in investigating the hybridization of new versions of FDO with different parameters. Furthermore, the performance of the hybridized version of FDO can be evaluated to assess the influence of objective evaluation.
- The performance of the proposed method can be further improved by hybridizing various optimization algorithms and implementing new fitness-dependent strategies to enhance convergence and reduce simulation time.
- This research can be extended to incorporate additional objective functions relevant to power systems in multi-objective optimization problems, such as demand response, economic cost minimization, harmonic reduction maximization, frequency regulation maximization, and environmental emission reduction.
- This work can be practically applied to real power systems, providing greater flexibility in addressing real-time issues. The proposed method could be adopted by generation companies (GENCOs) and distribution companies (DISCOs) with necessary modifications to their energy management systems. It is also advisable to investigate variability issues in real-time power networks.

Author Contributions: Conceptualization, M.U.R.; methodology, M.U.R.; software, M.U.R., S.A.M., A.D.; writing—original draft preparation, M.U.R.; supervision, S.A.M.; writing—review and editing, M.U.R., S.A.M., A.R.A., A.N.M.A., H.A. and A.D.; formal analysis, M.U.R., S.A.M., A.R.A.; validation, M.U.R., S.A.M., A.R.A., H.A., A.D. and A.N.M.A.; investigation, M.U.R., S.A.M., A.D., H.A. and A.R.A.; resources, M.U.R., A.R.A.; data curation, M.U.R. All authors have read and agreed to the published version of the manuscript.

Funding: This research received no external funding.

Data Availability Statement: The data supporting reported results are available in the manuscript.

Conflicts of Interest: The authors declare no conflict of interest.

Abbreviations

DG	Distributed Generator
RES	Renewable Energy Resources
PS	Power System
T&D	Transmission and Distribution
DN	Distribution Network
LLRI	Line Loss Reduction Index
LSF	Loss Sensitivity Factor
OPF	Optimal Power Flow
PLI	Power Loss Index
PLRI	Real Power Loss Reduction Index
QLI	Reactive Power Reduction Index
VSI	Voltage Sensitivity Indexes
CSI	Combined Sensitivity Indexes
GA	Genetic Algorithm
PSO	Particle Swarm Optimization
IPSO	Improved Particle Swarm Optimization
HGAIPSO	Hybrid Genetic Algorithm Improved Particle Swarm Optimization
FDO	Fitness-Dependent Optimizer
MFDO	Modified Fitness-Dependent Optimizer

References

1. Ackermann, T.; Andersson, G.; Söder, L. Distributed generation: A definition. *Electr. Power Syst. Res.* **2001**, *57*, 195–204. [CrossRef]
2. Adajah, Y.Y.; Thomas, S.; Haruna, M.S.; Anaza, S.O. Distributed Generation (DG): A review. In Proceedings of the 2021 1st International Conference on Multidisciplinary Engineering and Applied Science (ICMEAS), Abuja, Nigeria, 15–16 July 2021; pp. 1–5.
3. Zhang, J.; Cheng, H.; Wang, C. Technical and economic impacts of active management on distribution network. *Int. J. Electr. Power Energy Syst.* **2019**, *31*, 130–138. [CrossRef]
4. Popov, V.; Sikorsky, N.I.; Sikorsky, N.I. Optimal placement and sizing sources of distributed generation considering information uncertainty. In Proceedings of the IEEE 7th International Conference on Energy Smart Systems (ESS), Kyiv, Ukraine, 12–14 May 2020; pp. 253–257.
5. Rani, P.; Parkash, V.; Sharma, N.K. Technological aspects, utilization and impact on power system for distributed generation: A comprehensive survey. *Renew. Sustain. Energy Rev.* **2024**, *192*, 114257. [CrossRef]
6. Elseify, M.A.; Hashim, F.A.; Hussien, A.G.; Kamel, S. Single and multi-objectives based on an improved golden jackal optimization algorithm for simultaneous integration of multiple capacitors and multi-type DGs in distribution systems. *Appl. Energy* **2024**, *353*, 122054. [CrossRef]
7. Hassan, A.S.; Othman, E.A.; Bendary, F.M.; Ebrahim, M.A. Optimal integration of distributed generation resources in active distribution networks for techno-economic benefits. *Energy Rep.* **2020**, *6*, 3462–3471. [CrossRef]
8. Kumar, R.; Singh, B.K.; Singh, B. A Critical Review of Distributed Generations Planning in Distribution Networks for Improved System Performances. *J. Inst. Eng. Ser. B* **2024**, *105*, 1373–1427. [CrossRef]
9. Pothireddy KM, R.; Vuddanti, S.; Salkuti, S.R. Impact of demand response on optimal sizing of distributed generation and customer tariff. *Energies* **2022**, *15*, 190. [CrossRef]
10. Singh, S.; Singh, S. Advancements and challenges in integrating renewable energy sources into distribution grid systems: A comprehensive review. *J. Energy Resour. Technol.* **2024**, *146*, 090801. [CrossRef]
11. Yang, C.; Sun, Y.; Zou, Y.; Zheng, F.; Liu, S.; Zhao, B.; Wu, M.; Cui, H. Optimal power flow in distribution network: A review on problem formulation and optimization methods. *Energies* **2023**, *16*, 5974. [CrossRef]

12. Nassef, A.M.; Abdelkareem, M.A.; Maghrabie, H.M.; Baroutaji, A. Review of metaheuristic optimization algorithms for power systems problems. *Sustainability* **2023**, *15*, 9434. [CrossRef]
13. Siregar, R.H.; Away, Y.; Tarmizi; Akhyar. Minimizing Power Losses for Distributed Generation (DG) Placements by Considering Voltage Profiles on Distribution Lines for Different Loads Using Genetic Algorithm Methods. *Energies* **2023**, *16*, 5388. [CrossRef]
14. Gantayet, A.; Mohanty, S. An analytical approach for optimal placement and sizing of Distributed Generation based on a combined voltage stability index. In Proceedings of the 2015 IEEE Power, Communication and Information Technology Conference (PCITC), Bhubaneswar, India, 15–17 October 2015; pp. 762–767.
15. Bagherinasab, A.; Khalid, S.A.; Jahangere, H.; Kiani, M.J.; Yousef, A. Optimal placement in distribution network using shuffled frog leap algorithm. *EasyChair Prepr.* **2022**, 62–67.
16. Waseem, M.; Lin, Z.; Liu, S.; Zhang, Z.; Aziz, T.; Khan, D. Fuzzy compromised solution-based novel home appliances scheduling and demand response with optimal dispatch of distributed energy resources. *Appl. Energy* **2021**, *290*, 116761. [CrossRef]
17. Al-Ammar, E.A.; Farzana, K.; Waqar, A.; Aamir, M.; Haq, A.U.; Zahid, M.; Batool, M. ABC algorithm based optimal sizing and placement of DGs in distribution networks considering multiple objectives. *Aim Shams Eng. J. (ASEJ)* **2021**, *12*, 697–708. [CrossRef]
18. Farh, H.M.H.; Al-Shaalan, A.M.; Eltamaly, A.M.; Al-Shamma'A, A.A. A Novel Global Search Algorithm for Optimal Allocation and Sizing of Renewable Distributed Generation. *IEEE Access* **2020**, *8*, 27807–27820. [CrossRef]
19. Onlam, A.; Yodphet, D.; Chatthaworn, R.; Surawanitkun, C.; Siritaratiwat, A.; Khunkitti, P. Power Loss Minimization and Voltage Stability Improvement in Electrical Distribution System via Network Reconfiguration and Distributed Generation Placement Using Novel Adaptive Shuffled Frogs Leaping Algorithm. *Energies* **2019**, *12*, 553. [CrossRef]
20. Yammani, C.; Sydulu, M.; Matam, S.K. Optimal placement and sizing of DGs at various load conditions using Shuffled Bat algorithm. In Proceedings of the 2015 IEEE Power and Energy Conference at Illinois (PECI), Champaign, IL, USA, 20–21 February 2015; pp. 1–5.
21. Seker, A.A.; Hocaoglu, M.H. Artificial Bee Colony algorithm for optimal placement and sizing of distributed generation. In Proceedings of the 2013 8th International Conference on Electrical and Electronics Engineering (ELECO), Bursa, Turkey, 28–30 November 2013; pp. 127–131.
22. EL-Sayed, S.K. Optimal Location and Sizing of Distributed Generation for Minimizing Power Loss Using Simulated Annealing Algorithm. *J. Electr. Electron. Eng.* **2017**, *5*, 104–112.
23. Khan, H.; Choudhry, M.A. Implementation of Distributed Generation linear programming (LP) optimization algorithm for performance enhancement of distribution feeder under extreme load growth. *Int. J. Electr. Power Energy Syst.* **2020**, *32*, 985–997. [CrossRef]
24. Bhullar, S.; Ghosh, S. Optimal Integration of Distributed Generation Sources in Distribution Networks using Artificial bee Colony and Cuckoo Search base Algorithm. *Energies* **2021**, *11*, 628. [CrossRef]
25. Liaquat, S.; Fakhar, M.S.; Kashif, S.A.R.; Rasool, A.; Saleem, O.; Zia, M.F.; Padmanaban, S. Application of dynamically search space squeezed modified firefly algorithm to a novel short term economic dispatch of multi-generation systems. *IEEE Access* **2021**, *9*, 1918–1939. [CrossRef]
26. Liaquat, S.; Fakhar, M.S.; Kashif, S.A.R.; Saleem, O. Statistical analysis of accelerated PSO, firefly and enhanced firefly for economic dispatch problem. In Proceedings of the 2021 6th International Conference on Renewable Energy: Generation and Applications (ICREGA), Al Ain, United Arab Emirates, 2–4 February 2021; pp. 106–111.
27. Liaquat, S.; Fakhar, M.S.; Kashif, S.A.R.; Rasool, A.; Saleem, O.; Padmanaban, S. Performance analysis of APSO and firefly algorithm for short term optimal scheduling of multi-generation hybrid energy system. *IEEE Access* **2020**, *8*, 177549–177569. [CrossRef]
28. Alghamdi, A.S. A hybrid firefly–JAYA algorithm for the optimal power flow problem considering wind and solar power generations. *Appl. Sci.* **2022**, *12*, 7193. [CrossRef]
29. Sulaiman, M.H.; Mustaffa, Z.; Rashid, M.I.M. An application of teaching-learning-based optimization for solving the optimal power flow problem with stochastic wind and solar power generators. *Results Control Optim.* **2023**, *10*, 100187. [CrossRef]
30. Huang, J.; Gao, L.; Li, X. An effective teaching-learning-based cuckoo search algorithm for parameter optimization problems in structure designing and machining processes. *Appl. Soft Comput.* **2021**, *36*, 349–356. [CrossRef]
31. Zakaria, Y.Y.; Swief, R.A.; El-Amary, N.H.; Ibrahim, A.M. Optimal Distributed Generation Allocation and Sizing Using Genetic and Ant Colony Algorithms. *J. Phys. Conf. Ser.* **2020**, *1447*, 012023. [CrossRef]
32. Kaushik, E.; Prakash, V.; Mahela, O.P.; Khan, B.; Abdelaziz, A.Y.; Hong, J.; Geem, Z.W. Optimal placement of renewable energy generators using grid-oriented genetic algorithm for loss reduction and flexibility improvement. *Energies* **2022**, *15*, 1863. [CrossRef]
33. Kumar, B.A.; Jyothi, B.; Singh, A.R.; Bajaj, M.; Rathore, R.S.; Tuka, M.B. Hybrid genetic algorithm-simulated annealing based electric vehicle charging station placement for optimizing distribution network resilience. *Sci. Rep.* **2024**, *14*, 7637. [CrossRef]
34. Mohammad, M.; Nasab, M.A. PSO Based Multiobjective Approach for Optimal Sizing and Placement of Distributed Generation. *Res. J. Alied Sci. Eng. Technol.* **2017**, *10*, 842–847.
35. M'dioud, M.; Bannari, R.; Elkafazi, I. A novel PSO algorithm for DG insertion problem. *Energy Syst.* **2024**, *15*, 325–351. [CrossRef]
36. Ali, M.A.; Bhatti, A.R.; Rasool, A.; Farhan, M.; Esenogho, E. Optimal Location and Sizing of Photovoltaic-Based Distributed Generations to Improve the Efficiency and Symmetry of a Distribution Network by Handling Random Constraints of Particle Swarm Optimization Algorithm. *Symmetry* **2023**, *15*, 1752. [CrossRef]

37. Alanazi, A.; Alanazi, T.I. Multi-objective framework for optimal placement of distributed generations and switches in reconfigurable distribution networks: An improved particle swarm optimization approach. *Sustainability* **2023**, *15*, 9034. [CrossRef]
38. Sellami, R.; Farooq, S.H.; Rafik, N.E. An improved MOPSO algorithm for optimal sizing & placement of distributed generation: A case study of the Tunisian offshore distribution network (ASHTART). *Energy Rep.* **2022**, *8*, 6960–6975.
39. Eid, A. Allocation of distributed generations in radial distribution systems using adaptive PSO and modified GSA multi-objective optimizations. *Alex. Eng. J.* **2020**, *59*, 4771–4786. [CrossRef]
40. Rafi, V.; Dhal, P.K. Maximization savings in distribution networks with optimal location of type-I distributed generator along with reconfiguration using PSO-DA optimization techniques. *Mater. Today Proc.* **2020**, *33*, 4094–4100. [CrossRef]
41. Garg, H. A hybrid PSO-GA algorithm for constrained optimization problems. *Appl. Math. Comput.* **2016**, *274*, 292–305. [CrossRef]
42. Haghighi, H.; Sadati, S.H.; Dehghan, S.M.M.; Karimi, J. Hybrid form of particle swarm optimization and genetic algorithm for optimal path planning in coverage mission by cooperated unmanned aerial vehicles. *J. Aerosp. Technol. Manag.* **2020**, *12*, 1–10.
43. Satyanarayana, C.; Rao, K.N.; Bush, R.G.; Sujatha, M.S.; Roja, V.; Nageswara Prasad, T. Multiple DG placement and sizing in radial distribution system using genetic algorithm and particle swarm optimization. In *Computational Intelligence and Big Data Analytics: Applications in Bioinformatics*; Springer: Singapore, 2019; pp. 21–36.
44. Bala, R.; Ghosh, S. Applications, Optimal position and rating of DG in distribution networks by ABC–CS from load flow solutions illustrated by fuzzy-PSO. *Neural Comput.* **2019**, *31*, 489–507. [CrossRef]
45. Gomez-Gonzalez, M.; López, A.; Jurado, F. Optimization of distributed generation systems using a new discrete PSO and OPF. *Electr. Power Syst. Res.* **2012**, *84*, 174–180. [CrossRef]
46. Kumar, T.A.; Reddy, V.S.; Selvi, P.D.; Krishnakanth, B.; Sudeep, G. PSO and GSS algorithms are used to arrange DG optimally for voltage profile enhancement and loss reduction. *E3S Web Conf.* **2024**, *547*, 01013. [CrossRef]
47. Rajendran, A.; Narayanan, K. Optimal multiple installation of DG and capacitor for energy loss reduction and loadability enhancement in the radial distribution network using the hybrid WIPSO–GSA algorithm. *Int. J. Ambient Energy* **2018**, *41*, 129–141. [CrossRef]
48. Mirjalili, S.; Mirjalili, S.M.; Hatamlou, A. Multi-verse optimizer: A nature-inspired algorithm for global optimization. *Neural Comput. Appl.* **2022**, *27*, 495–513. [CrossRef]
49. Theo, W.L.; Lim, J.S.; Ho, W.S.; Hashim, H.; Lee, C.T. Review of distributed generation (DG) system planning and optimisation techniques: Comparison of numerical and mathematical modelling methods. *Renew. Sustain. Energy Rev.* **2017**, *67*, 531–573. [CrossRef]
50. Nayeripour, M.; Mahboubi-Moghaddam, E.; Aghaei, J.; Azizi-Vahed, A. Multi-objective placement and sizing of DGs in distribution networks ensuring transient stability using hybrid evolutionary algorithm. *Renew. Sustain. Energy Rev.* **2013**, *25*, 759–767. [CrossRef]
51. Salam, I.U.; Yousif, M.; Numan, M.; Zeb, K.; Billah, M. Optimizing Distributed Generation Placement and Sizing in Distribution Systems: A Multi-Objective Analysis of Power Losses, Reliability, and Operational Constraints. *Energies* **2023**, *16*, 5907. [CrossRef]
52. Akcakaya, M.; Nehorai, A. Adaptive MIMO radar design and detection in compound-Gaussian clutter. *IEEE Trans. Aerosp. Electron. Syst.* **2011**, *47*, 2200–2207. [CrossRef]
53. Heidari, A.A.; Heyrani, M.; Nakhkash, M. A dual-band circularly polarized stub loaded microstrip patch antenna for GPS applications. *Prog. Electromagn. Res.* **2009**, *92*, 195–208. [CrossRef]
54. Gorman, P.J.; Gregory, M.D.; Werner, D.H. Design of ultrawideband, aperiodic antenna arrays with the CMA evolutionary strategy. *IEEE Trans. Antennas Propag.* **2014**, *62*, 1663–1672. [CrossRef]
55. Wilking, B.A.; Lebofsky, M.J.; Rieke, G.H. The wavelength dependence of interstellar linear polarization-stars with extreme values of lambda/max. *Astron. J.* **1986**, *87*, 695–697. [CrossRef]
56. Sun, Y.; Wang, Z. Asynchronous and stochastic dimension updating and its application to parameter estimation for frequency modulated (FM) sound waves. In Proceedings of the 2015 IEEE International Conference on Progress in Informatics and Computing (PIC), Nanjing, China; 2015; pp. 583–587. [CrossRef]
57. Daraz, A.; Abdullah, S.; Mokhlis, H.; Haq, I.U.; Fareed, G.; Mansor, N.N. Fitness dependent optimizer-based automatic generation control of multi-source interconnected power system with non-linearities. *IEEE Access* **2020**, *8*, 100989–101003. [CrossRef]
58. Abbas, D.K.; Rashid, T.A.; Bacanin, K.H.; Alsadoon, A. Using fitness dependent optimizer for training multi-layer perceptron. *J. Internet Technol.* **2021**, *22*, 1575–1585. [CrossRef]
59. Daraz, A.; Malik, S.A.; Waseem, A.; Azar, A.T.; Haq, I.U.; Ullah, Z.; Aslam, S. Automatic generation control of multi-source interconnected power system using FOI-TD controller based FDO. *Energies* **2021**, *14*, 5867. [CrossRef]
60. Laghari, G.F.; Malik, S.A.; Daraz, A.; Ullah, A.; Alkhalifah, T.; Aslam, S. A numerical approach for solving nonlinear optimal control problems using the hybrid scheme of fitness dependent optimizer and Bernstein polynomials. *IEEE Access* **2022**, *10*, 50298–50313. [CrossRef]
61. Cikan, M.; Cikan, N.N. Optimum allocation of multiple type and number of DG units based on IEEE 123-bus unbalanced multi-phase power distribution system. *Int. J. Electr. Power Energy Systems.* **2023**, *144*, 108564. [CrossRef]
62. Selim, A.; Kamel, S.; Jurado, F. Efficient optimization technique for multiple DG allocation in distribution networks. *Appl. Soft Comput.* **2020**, *86*, 105938. [CrossRef]
63. Werkie, Y.; Kefale, H.A. Optimal allocation of distributed generation units in power distribution networks for voltage profile improvement and power losses minimization. *Int. J. Cogent Eng.* **2022**, *9*, 1. [CrossRef]

64. Chakravorty, M.; Das, D. Voltage stability analysis of radial distribution networks. *Int. J. Electr. Power Energy Syst.* **2001**, *23*, 129–135. [CrossRef]
65. Zhang, Q.; Li, H. MOEA/D: A Multiobjective Evolutionary Algorithm Based on Decomposition. *IEEE Trans. Evol. Comput.* **2011**, *11*, 712–731. [CrossRef]
66. Coello, C.A.C. Evolutionary multi-objective optimization:some current research trends and topics that remain to be explored. *Front. Comput. Sci. China* **2009**, *3*, 18–30. [CrossRef]
67. Alrajhi, H.; Daraz, A.; Alzahrani, A.; Babsail, H.; Alharbi, Y.; Alsharif, F.; Alattas, A.; Alshammari, K. Power Sharing Control Trends, Challenges, and Solutions in Multi-Terminal HVDC Systems: A Comprehensive Survey. *IEEE Access* **2024**, *12*, 69112–69129. [CrossRef]
68. Kumar, M.; Soomro, A.M.; Uddin, W.; Kumar, L. Optimal multi-objective placement and sizing of distributed generation in distribution system: A comprehensive review. *Energies* **2022**, *15*, 7850. [CrossRef]
69. Alrajhi, H. A novel synchronization method for seamless microgrid transitions. *Arab. J. Sci. Eng.* **2024**, *49*, 6867–6881. [CrossRef]
70. Selim, A.; Kamel, S.; Mohamed, A.A.; Elattar, E.E. Optimal allocation of multiple types of distributed generations in radial distribution systems using a hybrid technique. *Sustainability* **2021**, *13*, 6644. [CrossRef]
71. Abdullah, J.M.; Rashid, T.A. Fitness Dependent Optimizer: Inspired by the Bee Swarming Reproductive Process. *IEEE Access* **2019**, *7*, 43473–43486. [CrossRef]
72. Muhammed, D.A.; Saeed, S.A.M.; Rashid, T.A. Improved fitness dependent optimizer algorithm. *IEEE Access* **2019**, *8*, 19074–19088. [CrossRef]
73. Chiu, P.C.; Selamat, A.; Krejcar, O.; Kuok, K.K. Hybrid sine cosine and fitness dependent optimizer for global optimization. *IEEE Access* **2021**, *9*, 128601–128622. [CrossRef]
74. Mirjalili, S. SCA: A sine cosine algorithm for solving optimization problems. *Knowl.-Based Syst.* **2016**, *96*, 120–133. [CrossRef]
75. Qu, C.; Zeng, Z.; Dai, J.; Yi, Z.; He, W. A Modified sine-cosine algorithm based on neighborhood search and greedy levy mutation. *Comput. Intell. Neurosci.* **2018**, 4231647. [CrossRef]
76. Hamarashid, H.K.; Hassan, B.A.; Rashid, T.A. Modified-improved fitness dependent optimizer for complex and engineering problems. *Knowl.-Based Syst.* **2024**, *300*, 112098. [CrossRef]
77. Abdelaziz, M. Distribution network reconfiguration using a Genetic Algorithm with varying population size. *Electr. Power Syst. Res.* **2017**, *12*, 5–10. [CrossRef]
78. Jain, N.; Singh, S.N.; Srivastava, S.C. Particle Swarm Optimization Based Optimal Siting and Sizing of Multiple Distributed Generators. In Proceedings of the 16th National Power Systems Conference, Osmania, India; 2017; pp. 26–44.
79. Atteya, I.; Ashour, H.; Fahmi, A. Distribution network reconfiguration using modified particle swarm optimization. *IEEE Syst. J.* **2016**, *21*, 14–23.
80. Ntombela, M.; Musasa, K.; Leoaneka, M.C. Power Loss Minimization and Voltage Profile Improvement by System Reconfiguration, DG Sizing, and Placement. *Computation* **2022**, *10*, 180. [CrossRef]